A COMPARISON OF NUMERICAL ALGORITHMS FOR SOLUTION OF THE TRANSIENT STABILITY PROBLEM

by

E. Carter Gibson

Thesis submitted to the Graduate Faculty of the Virginia Polytechnic Institute and State University in partial fulfillment of the requirements for the degree of

Master of Science

in

Electrical Engineering

APPROVED:

L. L. Grigsby, Chairman

G. R. Powley

M. H. Hopkins

December 1977

Blacksburg, Virginia

ACKNOWLEDGMENTS

The author wishes to express his appreciation to Dr. L. L. Grigsby for serving as chairman of his graduate committee and for his guidance throughout the author's graduate study. Dr. Grigsby has served more as a friend then as an advisor and this is greatly appreciated.

The author wishes to thank Professor G. R. Powley and Dr. M. H. Hopkins for serving on his graduate committee. Thanks are also due Dr. T. E. Bechert who served on the author's committee before leaving VPI & SU. The financial assistance provided by the Energy Research Group is also appreciated.

Special thanks go to Cheryl West for typing this thesis. Her helpfulness, patience and friendship are greatly appreciated. Thanks are also due Lynda Caldwell and Sandy Crigger for their helpful attitude. Appreciation is expressed to the author's fellow graduate students for their many useful discussions.

Finally, the author wishes to express his appreciation to his wife, Rhonda, for her patience and understanding throughout his graduate work.

TABLE OF CONTENTS

TABLE OF CONTENTS, cont.

LIST OF FIGURES

LIST OF FIGURES, continued

LIST OF TABLES

LIST OF TABLES, continued

I. INTRODUCTION

With the United States' electric energy demand approximately doubling every ten years [2], the nation's utilities must also double their existing generation and transmission capabilities. This trend is leading to a vast, complex structure of interconnected power systems. With this growth in mind, it becomes easy to visualize the ever-increasing need of the transient stability analysis as an important tool in the planning and analysis of modern power systems. Our growing dependence on electric energy requires the use of the stability analysis to help avoid potentially dangerous situations such as those which accompanied the New York City blackout of 1977.

The need is present for a fast, accurate transient stability analysis. The present reliance on the digital computer, as well as the growth mentioned above, is impetus enough to warrant any research which may result in a time savings (and thus a cost savings) while producing accurate solutions.

The course taken in this thesis is to implement and compare five numerical algorithms for the solution of the differential equations contained in the stability problem. The five methods include: fourth-order Runge-Kutta; state transition; the trapezoidal rule of integration; Adams-Moulton predictor-corrector; and Hamming predictor-corrector. It is believed that, by comparing these algorithms, recommendations as to their relative merits can be made. It is hoped that the results of these comparisons will be of some benefit to the industry.

1.1 Literature Search

A great deal of literature is available on the topic of transient stability, particularly in the area of numerical solution techniques for solving the differential equations contained in the stability problem. In general, when a new algorithm is presented, it is compared to fourth-order Runge-Kutta, the industry-accepted standard solution technique.

The majority of recent work, in the area of numerical integration, has dealt with techniques classed as multistep algorithms [10], [12], [13]. Gross and Bergen [10] define a multistep method as one that uses "... the values of the dependent variable and its derivative at several points to compute the value at the next". Under the broad classification of multistep falls the algorithms classified as predictor-corrector techniques.

Perhaps the best known predictor-corrector algorithm uses the Adams-Bashforth predictor and the Adams-Moulton corrector [1], [4], [13]. The algorithm is implicit and requires that the corrector be iterated on until convergence. In [4] and [11] the Hamming predictor-corrector is presented. Hamming's method uses the same approach as the Adams-Moulton algorithm but has the advantage of intermediate steps which eliminate the need for iterating on the corrector. There are many other predictor-corrector methods available in the literature [4], [9] but the two mentioned seemed to receive the most attention.

Dommel and Sato [6] have taken another approach that warrants recognition. They solved the algebraic and differential equations simultaneously using the trapezoidal rule of integration to approximate the differential equations as algebraic equations. In converting the differential

equations to algebraic equations, Dommel and Sato assumed the differential equations to be linear over some time interval.

In most of the literature studied, a new method was presented, applied to a specific example, and compared to Runge-Kutta. It is felt that a more complete comparison is needed of several of the more noted algorithms. By applying five of the algorithms to several examples, a good, relative comparison can be made. Included in the algorithms studied is the state transition method. This method does not appear in any literature other than that found at VPI & SU [14], [17] but is believed to have great potential.

1.2 Scope of Investigation

The scope of this thesis is to present five numerical algorithms for the solution of the transient stability problem and to apply them to three examples. Included in the examples is the IEEE 14-bus system [18]. The results of the application of the algorithms to the examples will be compared.

In Chapter 2 the classical transient stability model will be developed. The algebraic model, including the generator and load models used, are derived. An explanation of the dynamic model, the swing equation, is presented, as well as the conversion of the equation to state variable form. Chapter 3 presents the five algorithms to be compared. A brief explanation and discussion of each of the methods is included. Information regarding derivation and approximate error is presented.

In Chapter 4 the three test systems and the results obtained from the five algorithms, when applied to the test systems, are presented.

Graphs of rotor angle versus time are used to compare the various algorithms. Conclusions and recommendations for further research are contained in Chapter 5. Included in the conclusions is a comparison of the results, including information about the relative accuracy, solution time and ease of programming of each method.

II. TRANSIENT STABILITY ANALYSIS

2.1 Introduction

The transient stability analysis (TSA) is an important tool used in the day-to-day analysis and, particularly, the planning of modern power systems. The TSA provides information, given a specific set of bus voltage, generation, and load data (a load flow solution), pertaining to the ability of the system under study to withstand a major disturbance. The type of disturbances referred to may be: a bus shorted to ground; a generator loss; a transmission line loss; a sudden load change; or a generator control failure.

The TSA utilizes two basic sets of equations for evaluating the system's performance under fault. The first set of equations contains representation of the algebraic portion of the system, i.e. buses, transmission lines, transformers, and equivalent machine and load representations. The second set consists of differential equations characterizing the machine's dynamic behavior. The desired detail of the analysis prescribes the number of differential equations required to adequately represent the machine and its corresponding controls. (The generator swing equation is used for this study as in many industry-related studies.)

The stability of the system is determined by solving the algebraic and differential equations simultaneously, for a particular fault, and observing the deviations of the rotor angular positions from their steady-state operating positions. If, from the TSA, it can be ascertained that the angular positions will settle to a new set of operating

points, then the system is stable. If, however, a new set of stable operating points is not reached, then the system will loss synchronism and be unstable [2], [9].

2.2 Algebraic Model

The basis for the formulation of the algebraic model is the prefault load flow. From the load flow, given system operating conditions, necessary for the calculation of the equivalent generator and load models, are obtained.

The classical TSA represents the generator as a Thevenin model, i.e. a voltage source in series with an equivalent generator admittance as shown in Figure 2.2.1a where

$\bar{V}_i$ = voltage at the ith bus;

$\bar{S}_{G_i}$ = complex power injected at the ith bus;

$\bar{I}_{G_i}$ = complex current injected at the ith bus;

$\bar{E}_i$ = emf of the ith generator;

$\bar{Y}_{G_i}$ = equivalent admittance of the ith generator.

The equivalent admittance is obtained from the transient reactance, x'_d, of the machine in question. The generator emf can be determined as

$$\bar{E}_i = \bar{V}_i^\circ + \frac{1}{\bar{Y}_{G_i}} \left(\frac{\bar{S}_{G_i}^\circ}{\bar{V}_i^\circ} \right)^* \qquad (2.2\text{-}1)$$

where the superscript zero denotes prefault values.

Using Norton's Theorem, we are able to convert the voltage source and series admittance into an equivalent current source in parallel with the admittance as seen in Figure 2.2.1b where

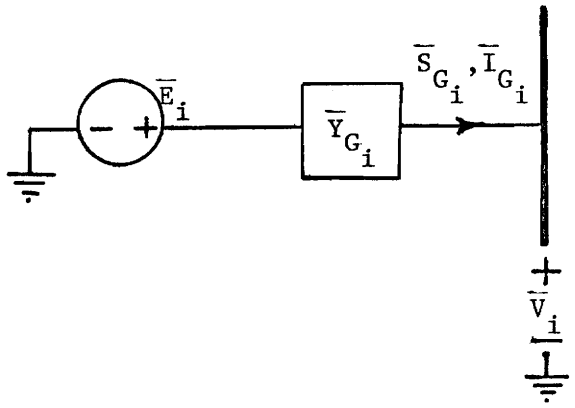

(a) Thevenin Equivalent Generator Model

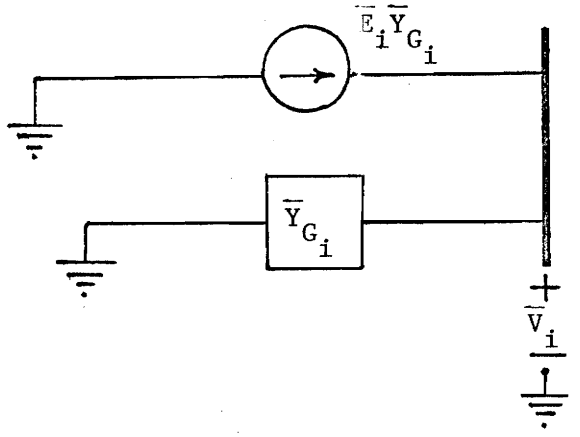

(b) Norton Equivalent Generator Model

Fig. 2.2.1 Generator Models

$$\bar{I}_{eq_i} = \bar{E}_i \bar{Y}_{G_i} . \tag{2.2-2}$$

There are two basic, classical approaches used to model loads. The first approach is to model the load as a constant impedance as seen in Figure 2.2.2a where

$\bar{S}_{D_j}$ = complex power drawn from the jth bus;

$\bar{I}_{D_j}$ = complex current drawn from the jth bus;

$\bar{Y}_{D_j}$ = equivalent admittance of the jth load.

The equivalent load admittance can be determined as

$$\bar{Y}_{D_j} = \frac{(\bar{S}^{\circ}_{D_j})^*}{|\bar{V}^{\circ}_j|^2} . \tag{2.2-3}$$

The second type of model is the constant current source model shown in Figure 2.2.2b. The current can be calculated as

$$\bar{I}_{D_j} = \left(\frac{\bar{S}^{\circ}_{D_j}}{\bar{V}^{\circ}_j} \right)^* . \tag{2.2-4}$$

Both types of load models are frequently used but for this study the constant impedance model is used exclusively.

Using the generator and load models explained above, we are now able to formulate the prefault algebraic model as

$$[\underline{\bar{Y}}_{bus} \text{ (PREFAULT)}] \, \underline{\bar{V}}_{bus} = \underline{\bar{I}}_{eq} \tag{2.2-5}$$

where

$\underline{\bar{Y}}_{bus}$ (PREFAULT) = prefault bus admittance matrix;

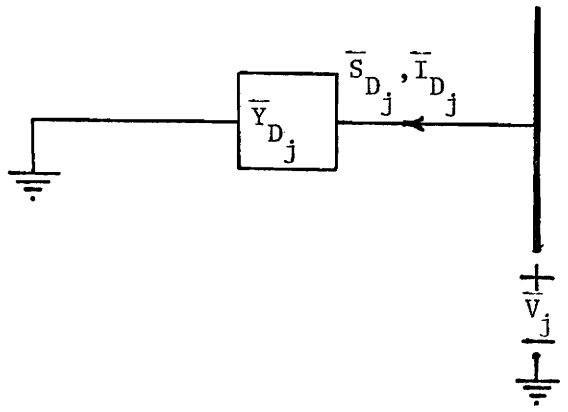

(a) Constant Impedance Load Model

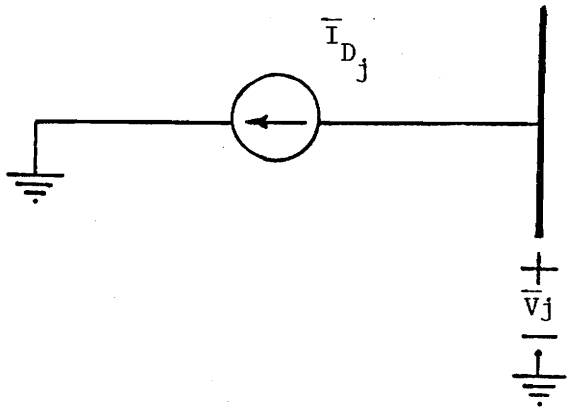

(b) Constant Current Load Model

Fig. 2.2.2 Load Models

$\bar{V}_{bus}$ = vector of bus voltages;

$\bar{I}_{eq}$ = vector of injected currents.

The prefault bus admittance matrix is obtained by adding the equivalent generator and load admittances to the appropriate diagonal entry of $\bar{Y}_{bus}$ obtained from the load flow.

When a major disturbance occurs within the system, modifications must be made to $\bar{Y}_{bus}$ (PREFAULT) to account for the fault. The modifications necessary to account for the three types of faults studied are:

i) for a shorted bus, a large admittance, of the order of -j1000 per unit, is added to the diagonal entry of $\bar{Y}_{bus}$ corresponding to the faulted bus;

ii) for a generator trip, the equivalent generator admittance must be removed from $\bar{Y}_{bus}$ and the injected current set equal to zero;

iii) for a line loss, the series and shunt parameters must be removed from any entry in $\bar{Y}_{bus}$ in which they appear.

Once $\bar{Y}_{bus}$ (PREFAULT) has been modified, Equation (2.2-5) is no longer satisfied and must be resolved for a new set of bus voltages. This faulted system can be expressed as

$$\bar{Y}^{f}_{bus}\bar{V}^{f}_{bus} = \bar{I}^{f}_{eq}. \qquad (2.2\text{-}6)$$

where the superscript "f" denotes faulted values.

2.3 Machine Model

The dynamic behavior of the system machines is described by a set of differential equations. The simplest representation is achieved

using the generator swing equation. The swing equation, describing the generator rotor dynamics, in per unit, is

$$\frac{d^2\delta_i}{dt^2} = \frac{-D_i \pi f^\circ}{H_i} \frac{d\delta_i}{dt} + \frac{\pi f^\circ}{H_i} (P_{T_i} - P_{E_i}) \qquad (2.3\text{-}1)$$

where

δ_i = rotor angle of ith machine;

D_i = damping constant of ith machine in MW-SEC/MVA-RAD;

π = 3.14159 RAD;

f° = nominal operating frequency in Hz;

H_i = inertia constant of ith machine in MW-SEC/MVA;

P_{T_i} = turbine power at bus i in per unit MW;

P_{E_i} = electrical power generated at bus i in per unit MW.

P_{E_i} can be expressed as

$$P_{E_i} = \mathrm{Re}[\bar{E}_i \bar{I}^*_{G_i}] \qquad (2.3\text{-}2a)$$

$$= \mathrm{Re}[\bar{Y}^*_{G_i} (|\bar{E}^\circ_i|^2 - |\bar{E}^\circ_i| \underline{/\delta i}\ \bar{V}^*_i)]. \qquad (2.3\text{-}2b)$$

One of the basic assumptions, when using the swing equation alone to represent the dynamics of the machine, is that P_T remains constant throughout the transient period. This restricts our period of study to approximately one second. If a longer period of study is desired, then a more complex set of differential equations must be used to model the machine.

The simplicity of the swing equation and the relatively accurate results it produces for short duration studies, makes it quite desirable. We can readily reduce (2.3-1) into two first-order equations expressed as

$$\dot{x}_{1_i} = x_{2_i} \tag{2.3-3a}$$

$$\dot{x}_{2_i} = \lambda_i x_{2_i} + \gamma_i P_{a_i} \tag{2.3-3b}$$

where

$$x_{1_i} = \delta_i$$

$$x_{2_i} = \frac{d\delta_i}{dt}$$

$$\gamma_i = \frac{\pi f^\circ}{H_i}$$

$$\lambda_i = -D_i \gamma_i$$

$$P_{a_i} = P_{T_i} - P_{E_i}.$$

(2.3-3a) and (2.3-3b) can be rewritten in state equation form as

$$\dot{\underline{x}}_i = \underline{A}_i \underline{x}_i + \underline{B}_i \underline{u}_i \tag{2.3-4}$$

where

$$\underline{A}_i = \begin{bmatrix} 0 & 1 \\ 0 & \lambda_i \end{bmatrix}$$

$$\underline{B}_i = \begin{bmatrix} 0 \\ \gamma_i \end{bmatrix}$$

$$\underline{u}_i = P_{a_i}$$

2.4 Solution Procedure

In the previous two sections we have developed an algebraic model and a dynamic model representing the system under study. The solution

of these two models results in the solution of the TSA. The difficulty in solving (2.2-6) and (2.3-4) is due to the coupling which exists between the two sets of equations.

From (2.2-2) we see that the equivalent current is a function of the rotor angle:

$$\bar{I}_{eq_i} = \bar{E}_i \bar{Y}_{G_i} = |\bar{E}_i^{\circ}| \underline{/\delta i}\ \bar{Y}_{G_i} \qquad (2.4\text{-}1)$$

While the magnitude of $\bar{E}_i$ is held constant throughout the transient period, the rotor angle is constantly changing.

The solution for the rotor angle, on the other hand, is dependent on the bus voltages from (2.2-6) and the previous value of the rotor angle.

The solution procedure that is adapted in this study, is an alternating solution technique. This procedure requires the independent solution of each set of equations, over some small time interval, while assuming that the coupled variables are clamped (remain constant) for that interval. This assumption is reasonable since the clamped variables, particularly the rotor angles, will change very little over some small interval.

Thus for some time interval, T, we solve (2.2-6) for $\underline{\bar{V}}_{bus}^{f}(nT)$. Using these values, we solve (2.3-4) for $\underline{x}[(n + 1)T]$. Since the state variables have now changed, we clamp $\underline{u}$ and resolve (2.2-6) for $\underline{\bar{V}}_{bus}^{f}$ $[(n + 1)T]$. This process continues until the solution period is completed.

The algebraic model is solved using LU decomposition (Appendix A). The LU decomposition method is chosen because it requires a retriangu-

larization of $\underline{\bar{Y}}^{f}_{bus}$ only when a network configuration change occurs. This lends itself to a speedy solution of the algebraic model.

The solution of the differential equations (2.3-4) poses the problem that we wish to examine in this thesis. There are many techniques available for solving (2.3-4). In the next chapter we will examine five of these methods and draw conclusions based on their performance as to which method yields the best results.

III. NUMERICAL ALGORITHMS

3.1 Introduction

In this chapter, a brief explanation about the derivation, application and error of each of the five numerical algorithms is given. Each of the algorithms is presented in general form as applied to

$$\dot{y} = f(x,y) \tag{3.1-1}$$

where

$$\dot{y} = \frac{dy}{dx}$$

f(x,y) = some function of x and y [1], [6], [15].

The algorithms are then presented in the specific form necessary for the solution of the state equations.

3.2 Runge-Kutta

The Runge-Kutta method is generally accepted as the standard solution technique for solving the machine swing equation. The method was developed to solve differential equations without evaluating higher order derivatives and without a loss of accuracy. The general form of Runge-Kutta is

$$y_{n+1} = y_n + h(a_1k_1 + a_2k_2 + \ldots + a_rk_r) \tag{3.2-1}$$

where h = step size;

a_i = constants to be evaluated;

k_i = values of the derivative, f(x,y), evaluated at a number of points in the interval $[x_n, x_{n+1}]$.

The formula (3.2-1) can be evaluated for any "r", thus producing any order of the method desired.

The most popular Runge-Kutta method used is fourth-order Runge-Kutta (r = 4). The constants are evaluated so that Runge-Kutta is identical with a Taylor series expansion in "r + 1" terms (for a detailed discussion concerning derivation see Conte and de Boor [1] or Jacquez [3]). This leads to the recursive formula

$$y_{n+1} = y_n + \frac{1}{6}(k_1 + 2k_2 + 2k_3 + k_4) \qquad (3.2\text{-}2)$$

where

$$k_1 = hf(x_n, y_n)$$

$$k_2 = hf(x_n + \frac{h}{2},\ y_n + \frac{k_1}{2})$$

$$k_3 = hf(x_n + \frac{h}{2},\ y_n + \frac{k_2}{2})$$

$$k_4 = hf(x_n + h,\ y_n + k_3).$$

Fourth-order Runge-Kutta is equivalent to a Taylor series expansion in five terms, thus the local truncation error is of the order (h^5).

Recall that we can write the swing equation for a single machine in state equation form as

$$\dot{\underline{x}} = \underline{A}\underline{x} + \underline{B}\underline{u} \qquad (3.2\text{-}3)$$

where

$$\underline{x} = \begin{bmatrix} \delta \\ \dot{\delta} \end{bmatrix}.$$

For the interval [n, n+1], the recursive solution for $\underline{x}$, using fourth-order Runge-Kutta, is best expressed with a flow chart as shown in Fig. 3.2.1, with

$\underline{x}_n^q$ = vector of state variables at step n (q = 0, 1, ..., 3 for all

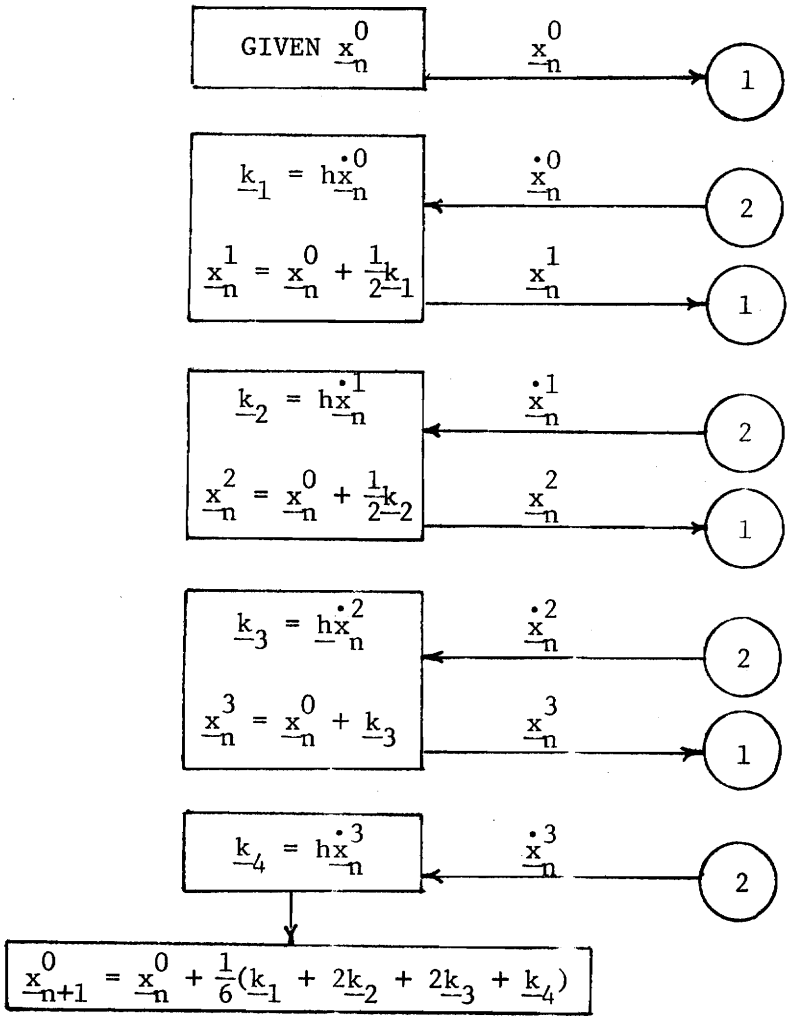

Fig. 3.2.1 Flow Chart for Solution of the Swing Equation of a Single Generator Using Fourth-Order Runge-Kutta

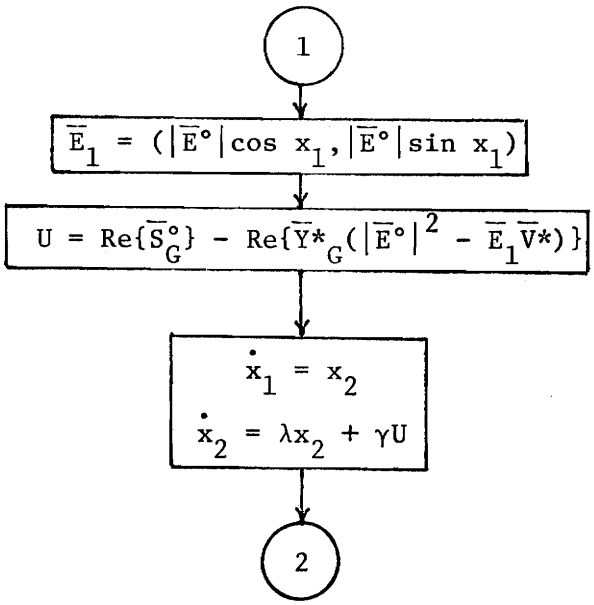

Fig. 3.2.1 Continued

variables);

$\dot{\underline{x}}^q_n$ = vector of derivatives of state variables at step n;

h = step size;

$\underline{k}_1, \ldots, \underline{k}_4$ = vector of constants defined by (3.2-2);

$\overline{E}_1$ = complex generator emf;

$|\overline{E}^\circ|$ = magnitude of prefault generator emf;

$\underline{u}$ = accelerating power (forcing function);

$|\overline{S}^\circ_G|$ = magnitude of prefault generated power;

$\overline{Y}^*_G$ = conjugate of generator admittance;

$\overline{V}^*$ = conjugate of complex bus voltage;

λ, γ = see (2.3-3).

Fig. 3.2.1 represents the calculations necessary to solve (3.2-3) for a single machine. From the flow chart and (3.2-2), it can be seen that four function evaluations must be made for each interval [n, n+1].

3.3 State Transition

The state equations (3.2-3) can be solved using the state transition method. Any system of the form (3.2-3) can be solved using

$$\underline{x}(t) = \underline{\phi}(t)\underline{x}(0) + \int_0^t \underline{\phi}(t-\tau)\underline{B}(\tau)\underline{u}(\tau)d\tau \qquad (3.3\text{-}1)$$

where $\underline{\phi}(t)$ = state transition matrix.

When solving the swing equation in state equation form, a recursive form of the state transition method is used. This recursive form on the interval [n, n+1], can be expressed as [19]

$$\underline{x}_{n+1} = \underline{\phi}(h)\underline{x}_n + \int_0^h \underline{\phi}(h-\tau)\underline{B}(\tau)\underline{u}_n d\tau \qquad (3.3\text{-}2)$$

where

h = step size.

Since (3.2-3) is a second-order set of equations, a closed form solution of the state transition matrix can be obtained using Laplace transforms as follows:

$$\underline{\phi}(s) = (s\underline{I} - \underline{A})^{-1} \tag{3.3-3}$$

where s = Laplace transform variable;

$\underline{I}$ = identity matrix;

$(\ )^{-1}$ = matrix inverse.

We must now evaluate $(s\underline{I} - \underline{A})$ and its inverse as

$$(s\underline{I} - \underline{A}) = \begin{bmatrix} s & -1 \\ 0 & s-\lambda \end{bmatrix} \tag{3.3-4}$$

$$(s\underline{I} - \underline{A})^{-1} = \begin{bmatrix} \frac{1}{s} & \frac{1}{s(s-\lambda)} \\ 0 & \frac{1}{s-\lambda} \end{bmatrix} \tag{3.3-5}$$

To determine $\underline{\phi}(h)$, we use the following

$$\underline{\phi}(h) = \mathcal{L}^{-1}\{\underline{\phi}(s)\} \tag{3.3-6}$$

which leads to

$$\underline{\phi}(h) = \begin{bmatrix} 1 & \frac{1}{\lambda}(e^{\lambda h}-1) \\ 0 & e^{\lambda h} \end{bmatrix} \tag{3.3-7}$$

Using the state transition matrix found in (3.3-7), we can now solve the integral which appears in (3.3-2) as

$$\underline{\theta}(h) = \int_0^h \begin{bmatrix} 1 & \frac{1}{\lambda}(e^{\lambda(h-\tau)}-1) \\ 0 & e^{\lambda(h-\tau)} \end{bmatrix} \begin{bmatrix} 0 \\ 1 \end{bmatrix} \gamma \underline{u} d\tau \tag{3.3-8}$$

Recall that one of the basic assumptions for solving the transient stability analysis is that $\gamma\underline{u}$ is constant for the interval [n, n+1]. We can therefore treat $\gamma\underline{u}$ as a unit step in (3.3-8). This yields the solution

$$\underline{\theta}(h) = \begin{bmatrix} \frac{1}{\lambda}\left[\frac{1}{\lambda}(e^{\lambda h}-1) - h\right] \\ \frac{1}{\lambda}\left[e^{\lambda h}-1\right] \end{bmatrix} \tag{3.3-9}$$

We can now formulate the solution of the state equations as [14]

$$\underline{x}_{n+1} = \underline{\phi}(h)\underline{x}_n + \underline{\theta}(h)\gamma\underline{u}_n \tag{3.3-10}$$

where

$$\underline{\phi}(h) = \begin{bmatrix} 1 & \frac{1}{\lambda}(e^{\lambda h}-1) \\ 0 & e^{\lambda h} \end{bmatrix}$$

$$\underline{\theta}(h) = \begin{bmatrix} \frac{1}{\lambda}\left[\frac{1}{\lambda}(e^{\lambda h}-1) - h\right] \\ \frac{1}{\lambda}\left[e^{\lambda h}-1\right] \end{bmatrix}.$$

The desirability of (3.3-10) is that $\underline{\phi}$ and $\underline{\theta}$ are dependent only on the step size, h. This means that the matrices must be evaluated only once for any given analysis, and the solution of the state equations reduces to a simple matrix multiplication. Also, since (3.3-10) is a closed form solution, we have eliminated the truncation error which inherently exists in other numerical integration techniques.

If the state equations representing the dynamic behavior of the machine were of an order greater than two, a closed form solution would be

difficult to obtain. If this is the case, the $\underline{\phi}$ and $\underline{\theta}$ matrices can be obtained using a power series expansion (See Grigsby [14]). This would lead to

$$\underline{\phi}(h) = \underline{I} + \underline{A}\underline{\xi}(h) \tag{3.3-11a}$$

$$\underline{\theta}(h) = \underline{\xi}(h)\underline{B} \tag{3.3-11b}$$

where

$$\underline{\xi}(h) = h\underline{I} + \frac{1}{2!}\underline{A}h^2 + \frac{1}{3!}\underline{A}^2h^3 + \ldots$$

$\underline{I}$ = identity matrix.

The series expansion for $\underline{\xi}(h)$ may be carried out until the addition of any new terms does not change the total series value by more than a specified tolerance.

3.4 Trapezoidal Rule

The trapezoidal rule can be used to evaluate any integral by approximating the area under the curve of the function to be integrated. To evaluate $\int_a^b f(x)dx$, we must first divide the function to be integrated into intervals, where each interval is

$$h = \frac{(b-a)}{n} \tag{3.4-1}$$

with h = interval (step) size;

a = lower integration limit;

b = upper integration limit;

n = total number of intervals;

as shown in Fig. 3.4.1 [15] where

$P_0, P_1, \ldots, P_n$ = values of f(x) at $x_0, x_1, \ldots, x_n$;

$y_0, y_1, \ldots, y_n$ = length of segment $aP_0, x_1P_1, \ldots, bP_n$.

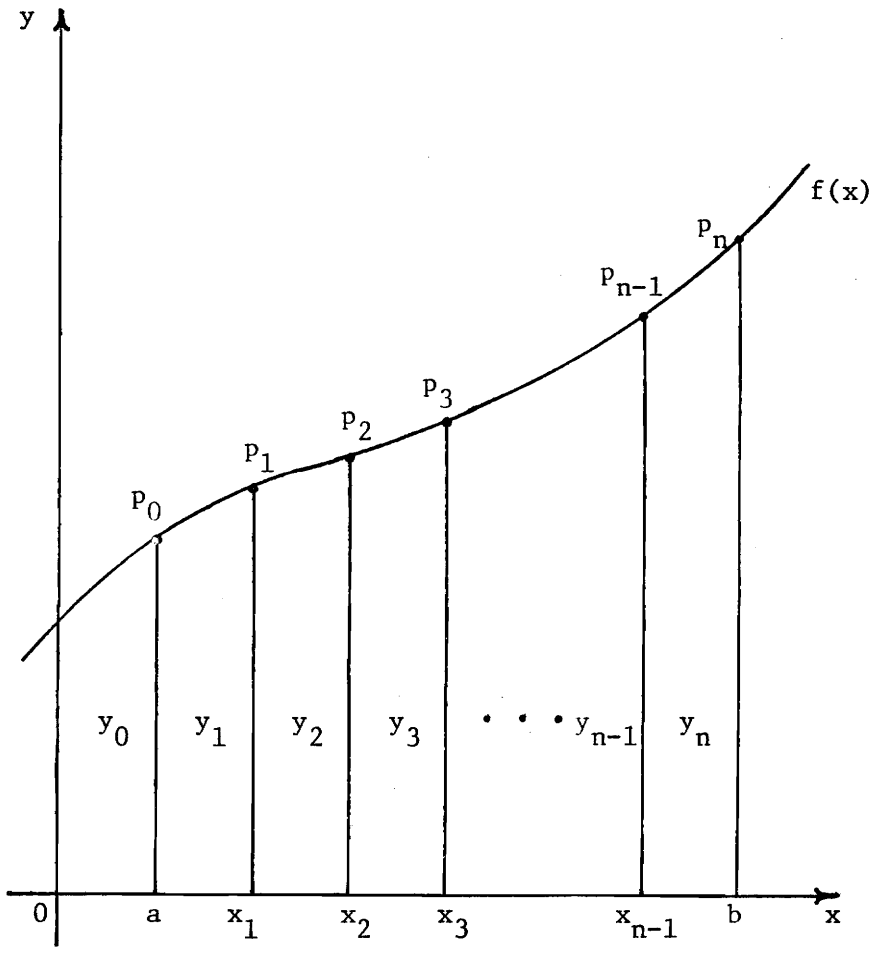

Fig. 3.4.1 Graphical Representation of the Trapezoidal Rule

The total integral may now be expressed as the sum of the integrals over each interval as

$$\int_a^b f(x)dx = \sum_{k=1}^{n} \int_{x_{k-1}}^{x_k} f(x)dx. \tag{3.4-2}$$

The value of each subintegral may be approximated as the area of a trapezoid. Thus

$$\int_a^{x_1} f(x)dx \simeq \frac{1}{2}(y_0 + y_1)h. \tag{3.4-3}$$

Using the trapezoidal rule, we can approximate the total integral as

$$\int_a^b f(x)dx = (\frac{1}{2}y_0 + y_1 + \ldots + y_{n-1} + \frac{1}{2}y_n)h. \tag{3.4-4}$$

The truncation error of (3.4-4) is of the order (h^3).

With the general form of the trapezoidal rule in mind, we can apply it to the state equation, (3.2-3), in the following manner. Given the recursive formula

$$\underline{x}_{n+1} = \underline{x}_n + \underline{A}\int_{nh}^{(n+1)h} \underline{x}d\tau + \underline{B}\int_{nh}^{(n+1)h} \underline{u}d\tau \tag{3.4-5}$$

we can approximate the solution as

$$\underline{x}_{n+1} = \underline{x}_n + \frac{h}{2}\underline{A}(\underline{x}_n + \underline{x}_{n+1}) + \frac{h}{2}\underline{B}(\underline{u}_n + \underline{u}_{n+1}) \tag{3.4-6}$$

(3.4-6) is a valid approximation to (3.4-5), provided that we assume $\underline{x}$ and $\underline{u}$ are linear over the interval [n, n+1].

We can see from (3.4-6) that the trapezoidal rule produces an implicit approximation since $\underline{u}_{n+1}$ is a function of $\underline{x}_{n+1}$. Because (3.4-6) is implicit, we must iterate on the equation for the solution of $\underline{x}_{n+1}$. The iterative method chosen to solve for $\underline{x}$, on the interval [n, n+1], is Gauss-Seidel since (3.4-6) is already in a Gauss-Seidel format.

Dommel and Sato [6] used (3.4-6) to approximate the state equations as algebraic equations. They then solved the algebraic network equations and the algebraic equations representing the state equations simultaneously. The procedure chosen in this study is to solve both sets of equations in an alternating fashion, as described in Section 2.4, rather than simultaneously.

3.5 Adams-Moulton Predictor-Corrector

The Adams-Moulton algorithm falls under the class of multistep methods. It utilizes the Adams-Bashforth predictor, and the Adams-Moulton corrector (see Conte and deBoor [1]).

Assume that we wish to integrate (3.1-1) on the interval $[x_n, x_{n+1}]$, we have

$$y_{n+1} = y_n + \int_{x_n}^{x_{n+1}} f(x,y(x))dx. \qquad (3.5\text{-}1)$$

Using the Newton backward formula we can obtain an interpolating polynomial at (m+1) points which approximates the integrand of (3.5-1). Incorporating this polynomial into (3.5-1) leads to the Adams-Bashforth predictor:

$$y^p_{n+1} = y_n + h(\gamma_0 f_n + \gamma_1 \Delta f_{n-1} + \ldots + \gamma_m \Delta^m f_{n-m}) \qquad (3.5\text{-}2)$$

where h = step size

$$\gamma_k = (-1)^k \int_0^1 \binom{-s}{k} ds$$

$$\Delta^k f_{n-k} = \text{kth difference of f.}$$

The most popular order of (3.5-2) used is fourth-order (m=3). With m=3, (3.5-2) becomes (with the differences already evaluated)

$$y^{p}_{n+1} = y_n + \frac{h}{24}(55f_n - 59f_{n-1} + 37f_{n-2} - 9f_{n-3}) \qquad (3.5\text{-}3)$$

where f_{n-k} = the function evaluated at the (n-k) time step; k=0, ..., 3. From (3.5-3) we see that, as with all multistep methods, values of the function, f, at previous steps, are required to solve for the (n+1) step (in this case, four values are needed).

The Adams-Moulton corrector is derived in a similar manner as the Adams-Bashforth predictor. The corrector formula utilizes the Newton backward formula to obtain an interpolating polynomial in (m+2) points. These (m+2) points include the predicted value of the (n+1) step obtained from (3.5-3). This leads to the Adams-Moulton corrector formula

$$y^{c}_{n+1} = y_n + h(\gamma'_o f_{n+1} + \gamma'_1 \Delta f_n + \ldots + \gamma'_{m+1} \Delta^{m+1} f_{n-m}) \qquad (3.5\text{-}4)$$

where

$$\gamma'_k = (-1)^k \int_0^1 \binom{1-s}{k} ds.$$

The fourth-order corrector (m=2) becomes

$$y^{c}_{n+1} = y_n + \frac{h}{24}(9f^{p}_{n+1} + 19f_n - 5f_{n-1} + f_{n-2}) \qquad (3.5\text{-}5)$$

where f^{p}_{n+1} = the function evaluated using y^{p}_{n+1}. The local truncation error of (3.5-3) and (3.5-5) is of the order (h^5).

From (3.5-3) and (3.5-5), we can see that the predictor is explicit while the corrector is implicit. This means that the corrector must be iterated on until convergence, or the step size, h, must be reduced. It is generally more desirable to reduce the step size than to iterate on the corrector.

The Adams-Moulton method has the ability to estimate the local discretization error [1] as

$$D_{n+1} \simeq \frac{-1}{14}(y^c_{n+1} - y^p_{n+1}) \tag{3.5-6}$$

where D_{n+1} = the discretization error of step (n+1).
By monitoring D_{n+1}, one can determine if the step size, h, is producing sufficient accuracy. Also, by observing D_{n+1}, one could build into the algorithm a variable step routine which automatically adjusts the step to increase or reduce accuracy as needed.

When the Adams-Moulton predictor-corrector method is applied to the state equations, we obtain the following

$$\underline{x}^p_{n+1} = \underline{x}_n + \frac{h}{24}(55\dot{\underline{x}}_n - 59\dot{\underline{x}}_{n-1} + 37\dot{\underline{x}}_{n-2} - 9\dot{\underline{x}}_{n-3}) \tag{3.5-7a}$$

$$\underline{x}^c_{n+1} = \underline{x}_n + \frac{h}{24}(9\dot{\underline{x}}^p_{n+1} + 19\dot{\underline{x}}_n - 5\dot{\underline{x}}_{n-1} + \dot{\underline{x}}_{n-2}) \tag{3.5-7b}$$

where $\underline{x}^p_{n+1}$ = predicted value of the state variables;

$\dot{\underline{x}}_{n-k}$ = derivative of the state variables at the (n-k) step, k = 0, ..., 3;

$\underline{x}^c_{n+1}$ = corrected value of the state variables;

$\dot{\underline{x}}^p_{n+1}$ = derivative of the state variables using the predicted value, $\underline{x}^p_{n+1}$.

As previously mentioned, the predictor, (3.5-7a), requires four previous values of $\dot{\underline{x}}$ to start the method. The method must be restarted whenever a system configuration change occurs, i.e. when a fault occurs

or is cleared. Fourth-order Runge-Kutta is used to obtain the four starting values since it produces highly accurate results.

3.6 Hamming Predictor-Corrector

The Hamming predictor-corrector algorithm, like Adams-Moulton, is a multistep method. It differs from Adams-Moulton in that it uses two intermediate calculations to eliminate the need for iterating on the corrector formula. To solve (3.3-1) on the interval $[x_n, x_{n+1}]$, we use the following general form:

(1) predict using

$$y^p_{n+1} = y_{n-3} + \frac{4h}{3}(2f_n - f_{n-1} + 2f_{n-2}) \qquad (3.6\text{-}1)$$

where y^p_{n+1} = predicted value at step (n+1);

h = step size;

y_{n-3} = final value at step (n-3);

f_{n-k} = function evaluated at step (n-k), k = 0, 1, 2;

(2) calculate an intermediate step using

$$y^m_{n+1} = y^p_{n+1} - \frac{112}{121}(y^p_n - y^c_n) \qquad (3.6\text{-}2)$$

where y^m_{n+1} = intermediate value at step (n+1);

(3) correct using

$$y^c_{n+1} = \frac{1}{8}[9y_n - y_{n-2} + 3h(f^m_{n+1} + 2f_n - f_{n-1})] \qquad (3.6\text{-}3)$$

where y^c_{n+1} = corrected value at step (n+1);

f^m_{n+1} = function evaluated using y^m_{n+1};

(4) calculate the final value using

$$y_{n+1} = y^c_{n+1} + \frac{9}{121}(y^p_{n+1} - y^c_{n+1}) \qquad (3.6\text{-}4)$$

where y_{n+1} = solution at step (n+1).

Upon examination of (3.6-1) - (3.6-4), we see that the implicit corrector, used in the Adams-Moulton algorithm, has been eliminated by modifying the predictor, (3.6-1), and the corrector, (3.6-3), and by adding two extra calculations, (3.6-2) and (3.6-4). Since the Hamming method is noniterative, it has been found to be more stable than iterative predictor-corrector methods [11].

A measure of the error of the Hamming algorithm on the interval [n, n+1] can be obtained as

$$D_{n+1} \simeq |y^c_{n+1} - y^p_{n+1}| \qquad (3.6\text{-}5)$$

where D_{n+1} = the approximate error of step (n+1).

When we apply the Hamming predictor-corrector to the state equations, we obtain the following form:

$$\underline{x}^p_{n+1} = \underline{x}_{n-3} + \frac{4h}{3}(2\dot{\underline{x}}_n - \dot{\underline{x}}_{n-1} + 2\dot{\underline{x}}_{n-2}) \qquad (3.6\text{-}6a)$$

$$\underline{x}^m_{n+1} = \underline{x}^p_{n+1} - \frac{112}{121}(\underline{x}^p_n - \underline{x}^c_n) \qquad (3.6\text{-}6b)$$

$$\underline{x}^c_{n+1} = \frac{1}{8}[9\underline{x}_n - \underline{x}_{n-2} + 3h(\dot{\underline{x}}^m_{n+1} + 2\dot{\underline{x}}_n - \dot{\underline{x}}_{n-1})] \qquad (3.6\text{-}6c)$$

$$\underline{x}_{n+1} = \underline{x}^c_{n+1} + \frac{9}{121}(\underline{x}^p_{n+1} - \underline{x}^c_{n+1}). \qquad (3.6\text{-}6d)$$

The Hamming algorithm also requries four starting values at the beginning of the analysis, and at every discontinuity, within the analysis, due to switching operations. As with the Adams-Moulton algorithm,

fourth-order Runge-Kutta was used to obtain the starting values.

3.7 Summary of the Numerical Algorithms

In this section, the five numerical algorithms, as applied to the swing equations, will be repeated for quick reference.

Recall that for this study, the methods are used to solve the second-order system

$$\dot{\underline{x}} = \underline{A}\underline{x} + \underline{B}\underline{u} \tag{3.7-1}$$

The five algorithms as applied to (3.7-1) are:

(1) fourth-order Runge-Kutta

$$\underline{x}_{n+1} = \underline{x}_n + \frac{1}{6}(\underline{k}_1 + 2\underline{k}_2 + 2\underline{k}_3 + \underline{k}_4) \tag{3.7-2}$$

where $\underline{k}_1, \ldots, \underline{k}_4$ are given in Fig. 3.1.1;

(2) state transition

$$\underline{x}_{n+1} = \underline{\phi}(h)\underline{x}_n + \underline{\theta}(h)\,\underline{u}_n \tag{3.7-3}$$

where

$$\underline{\phi}(h) = \begin{bmatrix} 1 & \frac{1}{\lambda}(e^{\lambda h}-1) \\ 0 & e^{\lambda h} \end{bmatrix}$$

$$\underline{\theta}(h) = \begin{bmatrix} \frac{1}{\lambda}[\frac{1}{\lambda}(e^{\lambda h}-1) - h] \\ \frac{1}{\lambda}(e^{\lambda h}-1) \end{bmatrix};$$

(3) trapezoidal rule

$$\underline{x}_{n+1} = \underline{x}_n + \frac{h}{2}\underline{A}(\underline{x}_n + \underline{x}_{n+1}) + \frac{h}{2}\underline{B}(\underline{u}_n + \underline{u}_{n+1}); \tag{3.7-4}$$

(4) Adams-Moulton predictor-corrector

$$\underline{x}^{p}_{n+1} = \underline{x}_n + \frac{h}{24}(55\dot{\underline{x}}_n - 59\dot{\underline{x}}_{n-1} + 37\dot{\underline{x}}_{n-2} - 9\dot{\underline{x}}_{n-3}) \qquad (3.7\text{-}5a)$$

$$\underline{x}^{c}_{n+1} = \underline{x}_n + \frac{h}{24}(9\dot{\underline{x}}^{p}_{n+1} + 19\dot{\underline{x}}_n - 5\dot{\underline{x}}_{n-1} + \dot{\underline{x}}_{n-2}); \qquad (3.7\text{-}5b)$$

(5) Hamming predictor-corrector

$$\underline{x}^{p}_{n+1} = \underline{x}_{n-3} + \frac{4h}{3}(2\dot{\underline{x}}_n - \dot{\underline{x}}_{n-1} + 2\dot{\underline{x}}_{n-2}) \qquad (3.7\text{-}6a)$$

$$\underline{x}^{m}_{n+1} = \underline{x}^{p}_{n+1} - \frac{112}{121}(\underline{x}^{p}_n - \underline{x}^{c}_n) \qquad (3.7\text{-}6b)$$

$$\underline{x}^{c}_{n+1} = \frac{1}{8}[9\underline{x}_n - \underline{x}_{n-2} + 3h(\dot{\underline{x}}^{m}_{n+1} + 2\dot{\underline{x}}_n - \dot{\underline{x}}_{n-1})] \qquad (3.7\text{-}6c)$$

$$\underline{x}_{n+1} = \underline{x}^{c}_{n+1} + \frac{9}{121}(\underline{x}^{p}_{n+1} - \underline{x}^{c}_{n+1}). \qquad (3.7\text{-}6d)$$

The various variable definitions are given in the section in which the algorithm is discussed.

IV. TEST SYSTEMS AND RESULTS

4.1 Introduction

In this chapter, the three test systems that the five numerical algorithms were applied to and the results obtained are presented. A system diagram and the necessary input data for each system is given. The results obtained from applying the five algorithms, using different step sizes, are presented in tabular and graphical form.

Since it would be impractical to present the results obtained at each time step for every case, the values of rotor angle at specific time intervals, namely .25, .50, .75, and 1.00 seconds, for each case are presented in a table. Also given is a comparison of compilation and execution times for each case. The times were obtained from the IBM 370 computer on which all cases were performed.

Plots of rotor angle versus time for machine one (δ_1) are used to compare the different algorithms, using different step sizes. For these plots, the algorithms will be denoted using the following legend:

RK = fourth-order Runge-Kutta;

ST = state transition;

TRAP = the trapezoidal rule;

AM = Adams-Moulton predictor-corrector;

HAM = Hamming predictor-corrector.

For simplicity, the value of the step size used will be given as 1/h. Thus, for a step of 1/120 (.0083), the value presented on the plots will be 120.

4.2 Test System I

The first test system analyzed is the nine-bus system that appears in Anderson and Fouad's book Power System Control and Stability [8]. A system diagram of the nine-bus system appears in Fig. 4.2.1. Given system line and transformer data appears in Table (4.2.1). Necessary generator data appears in Table (4.2.2) and the system's prefault bus data is presented in Table (4.2.3).

The type of fault analyzed is a short near the end of line 5-7 that could be approximated by shorting bus 7. The fault was cleared after 5 cycles by removing line 5-7. The five numerical algorithms, using various step sizes, were applied to this system.

In Table (4.2.4), a comparison of compilation and execution times is presented. A comparison of the rotor angle values obtained from the various cases, for the four time intervals given in Section 4.1, appears in Tables (4.2.5)-(4.2.8).

Plots comparing the swing curve of machine one for the five algorithms, using various step sizes, appear in Figs. 4.2.2-4.2.5. In Fig. 4.2-6 the swing curves for all three machine, obtained using state transition ($h = 1/120$), are presented.

4.3 Test System II

In this section, the system under study is the IEEE fourteen-bus system (Fig. 4.3.1)[18]. The system line data is tabulated in Table (4.3.1). Necessary transformer and generator data appear in Table (4.3.2) and prefault bus data is presented in Table (4.3.3).

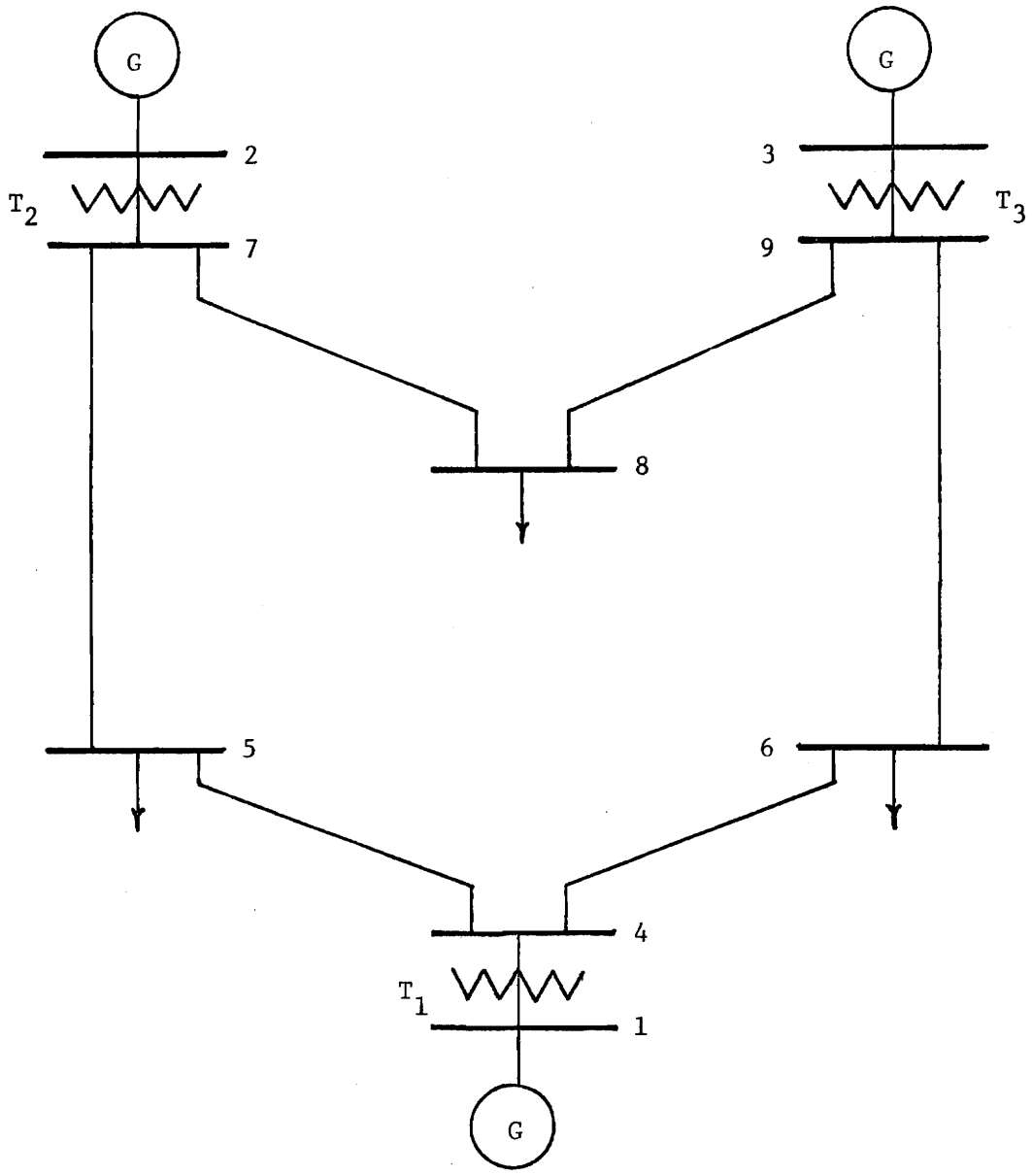

Fig. 4.2.1 Test System I

Anderson & Fouad 9-Bus System

TABLE 4.2.1 ANDERSON & FOUAD 9-BUS SYSTEM
LINE AND TRANSFORMER DATA

LINE NUMBER	STARTING BUS	ENDING BUS	RESISTANCE PER UNIT*	REACTANCE PER UNIT*	LINE CHARGING PER UNIT**
1	4	5	.0100	.0850	.0880
2	4	6	.0170	.0920	.0790
3	5	7	.0320	.1610	.1530
4	6	9	.0390	.1700	.1790
5	7	8	.0085	.0720	.0745
6	8	9	.0119	.1008	.1045

(a) LINE DATA

TRANSFORMER NUMBER	STARTING BUS	ENDING BUS	RESISTANCE PER UNIT*	REACTANCE PER UNIT*	TURNS RATIO
1	1	4	0.0	.0576	1.0
2	2	7	0.0	.0625	1.0
3	3	9	0.0	.0586	1.0

(b) TRANSFORMER DATA

*All per-unit values are on a 100 MVA base

**Line charging is one half of total charging (B/2)

TABLE 4.2.2 ANDERSON & FOUAD 9-BUS SYSTEM
GENERATOR DATA

GENERATOR NUMBER	INERTIA CONSTANT* MW-SEC/MVA	DAMPING COEFFICIENT MW-SEC/MVA-RAD	TRANSIENT REACTANCE PER UNIT*
1	23.64	0.0	.0608
2	6.40	0.0	.1198
3	3.01	0.0	.1813

*Based on a 100 MVA base

TABLE 4.2.3 ANDERSON & FOUAD 9-BUS SYSTEM
PREFAULT BUS DATA

BUS NUMBER	GENERATOR NUMBER	BUS VOLTAGES		GENERATION		DEMAND	
		MAGNITUDE PER-UNIT	ANGLE DEGREES	REAL MW	REACTIVE MVAR	REAL MW	REACTIVE MVAR
1	1	1.040	0.0	71.6	27.0	0.0	0.0
2	2	1.025	9.3	163.0	6 .7	0.0	0.0
3	3	1.025	4.7	85.0	-10.9	0.0	0.0
4		1.026	-2.2			0.0	0.0
5		0.996	-4.0			125.0	50.0
6		1.013	-3.7			90.0	30.0
7		1.026	3.7			0.0	0.0
8		1.016	0.7			100.0	35.0
9		1.032	2.0			0.0	0.0

TABLE 4.2.4 COMPARISON OF COMPIIATION AND EXECUTION TIMES FOR ANDERSON & FOUAD'S 9-BUS SYSTEM

METHOD	STEP SIZE (1/h)	COMPILATION TIME SECONDS	EXECUTION TIME SECONDS
RUNGE-KUTTA	60	1.73	7.21
RUNGE-KUTTA	120	1.87	14.45
RUNGE-KUTTA	240	1.93	28.25
RUNGE-KUTTA	360	1.90	41.80
STATE TRANSITION	60	1.64	5.94
STATE TRANSITION	120	1.82	12.50
STATE TRANSITION	360	1.92	35.20
TRAPEZOIDAL	60	1.96	9.77
TRAPEZOIDAL	120	1.88	17.27
TRAPEZOIDAL	240	1.70	27.70
TRAPEZOIDAL	360	2.05	44.13
ADAMS-MOULTON	120	1.98	15.52
ADAMS-MOULTON	240	1.92	27.48
ADAMS-MOULTON	360	1.80	39.08
HAMMING	120	2.09	16.53
HAMMING	240	1.92	29.10
HAMMING	360	1.89	43.93

TABLE 4.2.5 COMPARISON OF ROTOR ANGLES (δ) FOR ANDERSON & FOUAD'S 9-BUS SYSTEM AT t = .25 SECONDS

METHOD	STEP SIZE (1/h)	δ_1 DEGREES	δ_2 DEGREES	δ_3 DEGREES
RUNGE-KUTTA	60	3.00	62.45	39.25
RUNGE-KUTTA	120	3.26	65.41	41.72
RUNGE-KUTTA	240	3.41	67.06	43.12
RUNGE-KUTTA	360	3.47	67.64	43.62
STATE TRANSITION	60	3.28	69.59	44.97
STATE TRANSITION	120	3.43	69.22	44.82
STATE TRANSITION	360	3.53	68.97	44.71
TRAPEZOIDAL	60	2.98	62.23	39.08
TRAPEZOIDAL	120	3.26	65.34	41.67
TRAPEZOIDAL	240	3.41	67.04	43.11
TRAPEZOIDAL	360	3.47	67.63	43.61
ADAMS-MOULTON	120	3.08	63.26	39.88
ADAMS-MOULTON	240	3.29	65.63	41.89
ADAMS-MOULTON	360	3.37	66.59	42.72
HAMMING	120	3.68	63.24	39.87
HAMMING	240	3.29	65.62	41.89
HAMMING	360	3.37	66.59	42.72

TABLE 4.2.6 COMPARISON OF ROTOR ANGLES (δ) FOR ANDERSON & FOUAD'S 9-BUS SYSTEM AT t = .50 SECONDS

METHOD	STEP SIZE (1/h)	δ_1 DEGREES	δ_2 DEGREES	δ_3 DEGREES
RUNGE-KUTTA	60	15.69	81.07	60.15
RUNGE-KUTTA	120	18.83	91.88	69.03
RUNGE-KUTTA	240	20.68	98.66	74.69
RUNGE-KUTTA	360	21.35	101.18	76.80
STATE TRANSITION	60	21.80	108.84	83.27
STATE TRANSITION	120	22.29	107.73	82.33
STATE TRANSITION	360	22.61	107.01	81.72
TRAPEZOIDAL	60	15.50	81.09	60.13
TRAPEZOIDAL	120	18.77	91.86	69.01
TRAPEZOIDAL	240	20.67	98.65	74.68
TRAPEZOIDAL	360	21.34	101.17	76.79
ADAMS-MOULTON	120	16.17	82.35	61.15
ADAMS-MOULTON	240	18.97	92.26	69.34
ADAMS-MOULTON	360	20.11	96.46	72.84
HAMMING	120	16.16	82.32	61.12
HAMMING	240	18.96	92.25	69.33
HAMMING	360	20.10	96.45	72.83

TABLE 4.2.7 COMPARISON OF ROTOR ANGLES (δ) FOR ANDERSON & FOUAD'S 9-BUS SYSTEM AT t = .75 SECONDS

METHOD	STEP SIZE (1/h)	δ_1 DEGREES	δ_2 DEGREES	δ_3 DEGREES
RUNGE-KUTTA	60	41.95	76.65	61.85
RUNGE-KUTTA	120	53.74	89.81	74.26
RUNGE-KUTTA	240	61.20	99.60	83.15
RUNGE-KUTTA	360	63.96	103.55	86.69
STATE TRANSITION	60	69.89	115.24	95.87
STATE TRANSITION	120	69.95	113.95	95.34
STATE TRANSITION	360	69.95	113.18	95.03
TRAPEZOIDAL	60	41.68	76.85	61.88
TRAPEZOIDAL	120	53.63	89.87	74.26
TRAPEZOIDAL	240	61.17	99.61	83.15
TRAPEZOIDAL	360	63.94	103.55	86.69
ADAMS-MOULTON	120	43.07	77.69	62.94
ADAMS-MOULTON	240	54.08	90.18	74.63
ADAMS-MOULTON	360	58.74	96.20	80.10
HAMMING	120	43.04	77.66	62.91
HAMMING	240	54.07	90.17	74.62
HAMMING	360	58.73	96.19	80.10

TABLE 4.2.8 COMPARISON OF ROTOR ANGLES (δ) FOR ANDERSON & FOUAD'S 9-BUS SYSTEM AT t = 1.00 SECONDS

METHOD	STEP SIZE (1/h)	δ_1 DEGREES	δ_2 DEGREES	δ_3 DEGREES
RUNGE-KUTTA	60	62.49	85.28	77.22
RUNGE-KUTTA	120	85.29	100.17	95.38
RUNGE-KUTTA	240	101.29	111.10	108.46
RUNGE-KUTTA	360	107.55	115.51	113.66
STATE TRANSITION	60	124.67	123.61	126.49
STATE TRANSITION	120	123.21	124.79	126.07
STATE TRANSITION	360	122.25	125.55	125.81
TRAPEZOIDAL	60	62.42	84.95	77.01
TRAPEZOIDAL	120	85.23	100.05	95.28
TRAPEZOIDAL	240	101.26	111.06	108.42
TRAPEZOIDAL	360	107.53	115.49	113.64
ADAMS-MOULTON	120	64.06	86.30	78.41
ADAMS-MOULTON	240	85.81	100.51	95.78
ADAMS-MOULTON	360	95.77	107.27	103.90
HAMMING	120	64.61	86.27	78.38
HAMMING	240	85.80	100.50	95.77
HAMMING	360	95.76	107.26	103.89

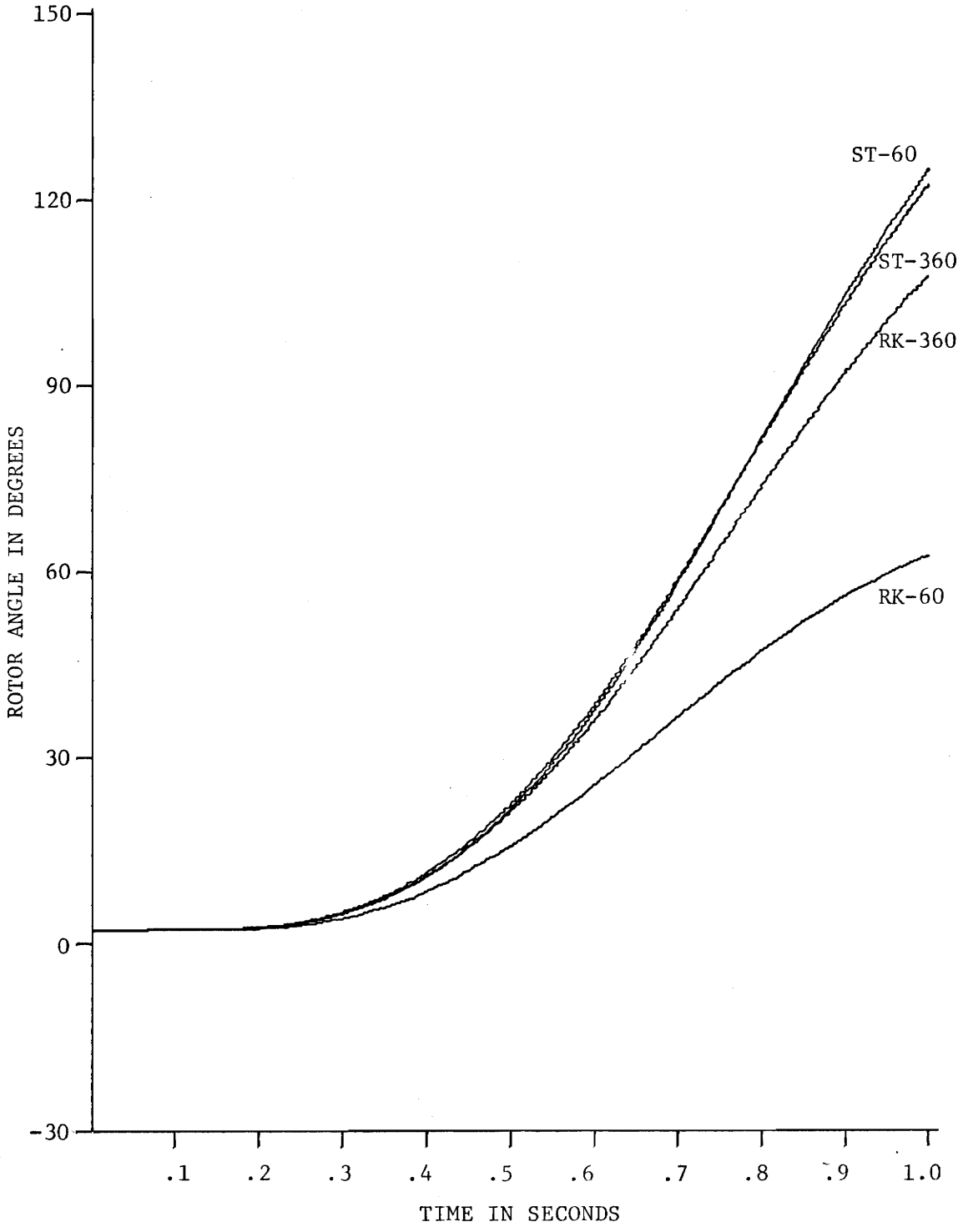

Fig. 4.2.2. Comparison of State Transition and Runge-Kutta Anderson and Fouad's 9-Bus System (δ_1)

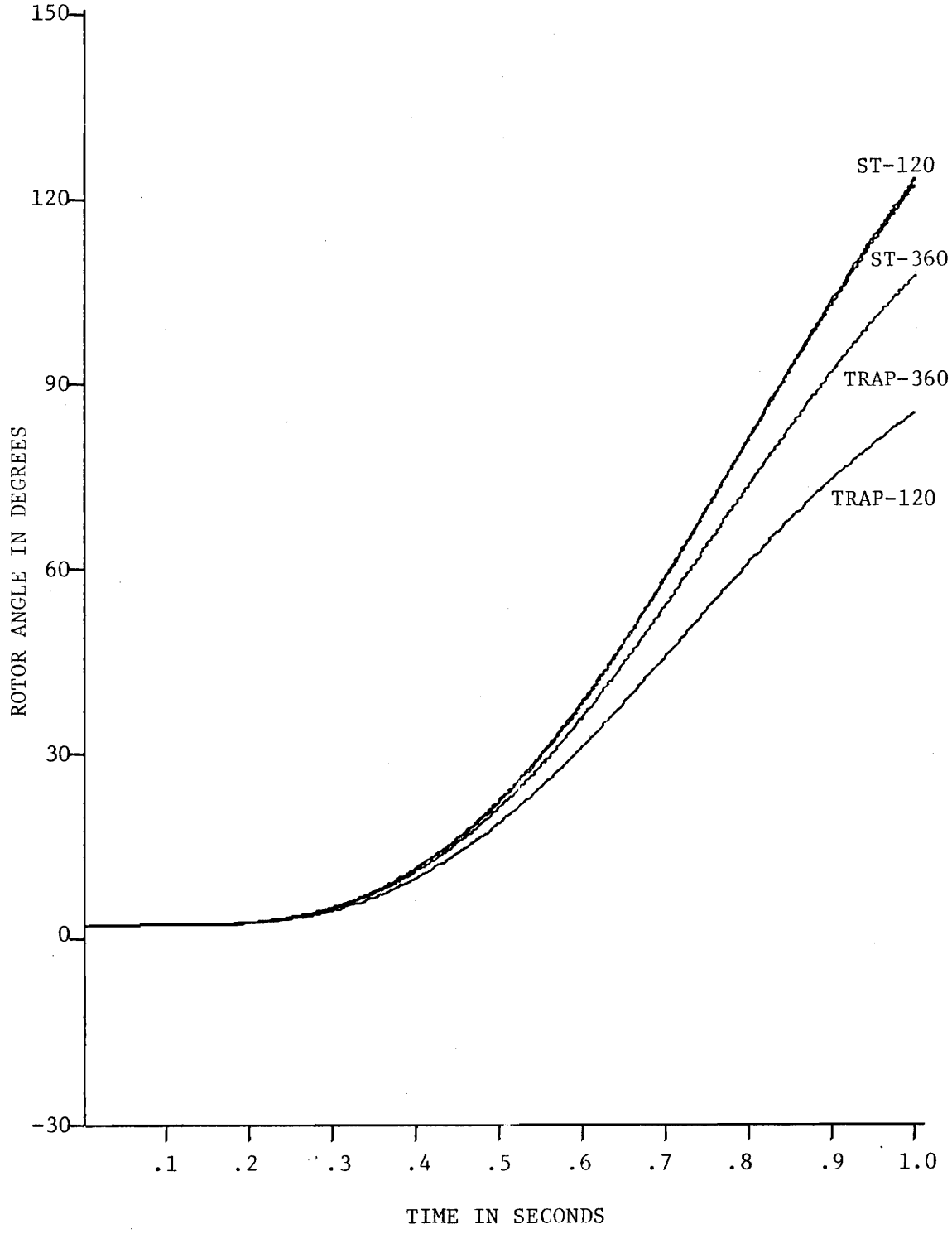

Fig. 4.2.3 Comparison of State Transition and the Trapezoidal Rule Anderson and Fouad's 9-Bus System (δ_1)

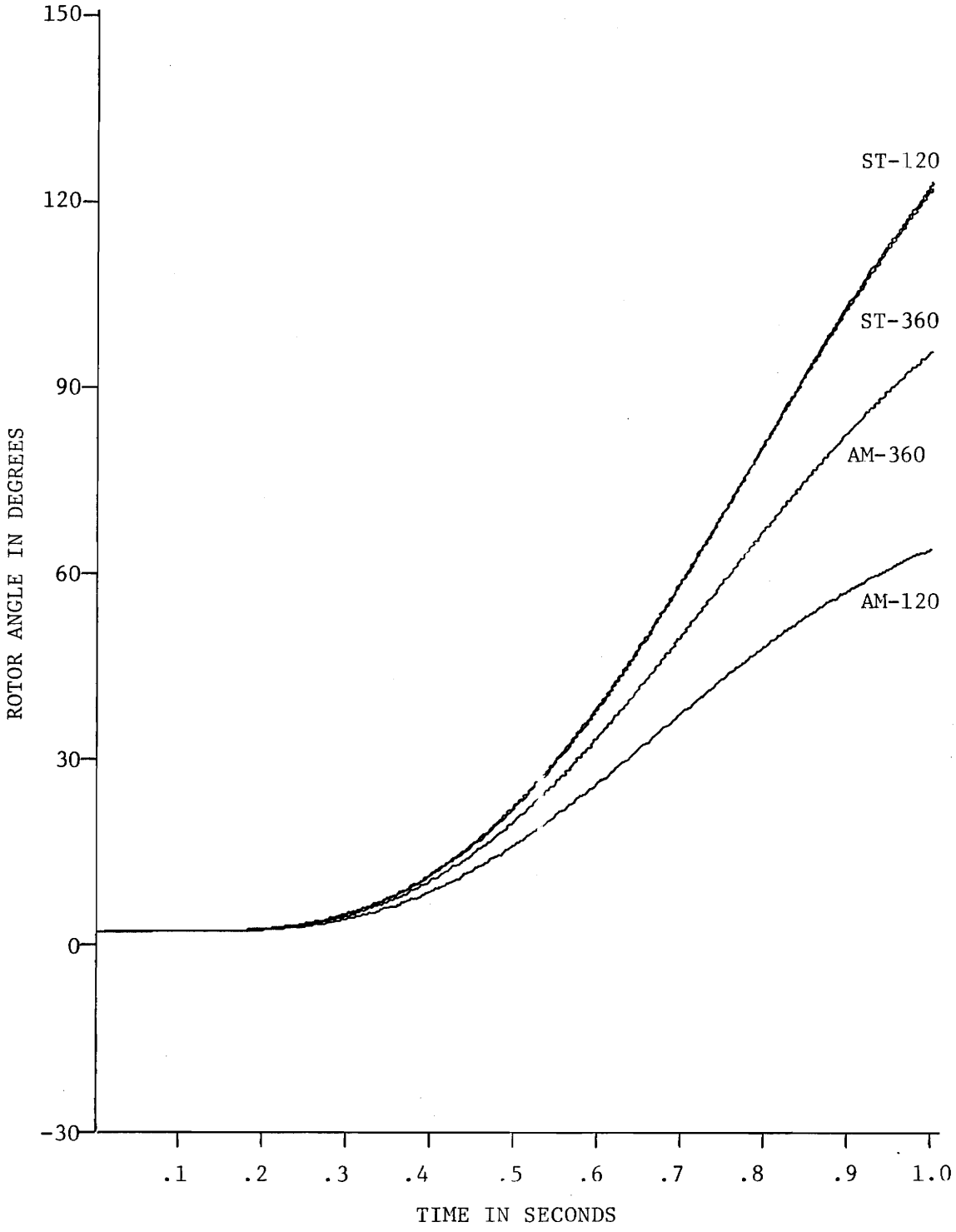

Fig. 4.2.4 Comparison of State Transition and Adams-Moulton Anderson and Fouad's 9-Bus System (δ_1)

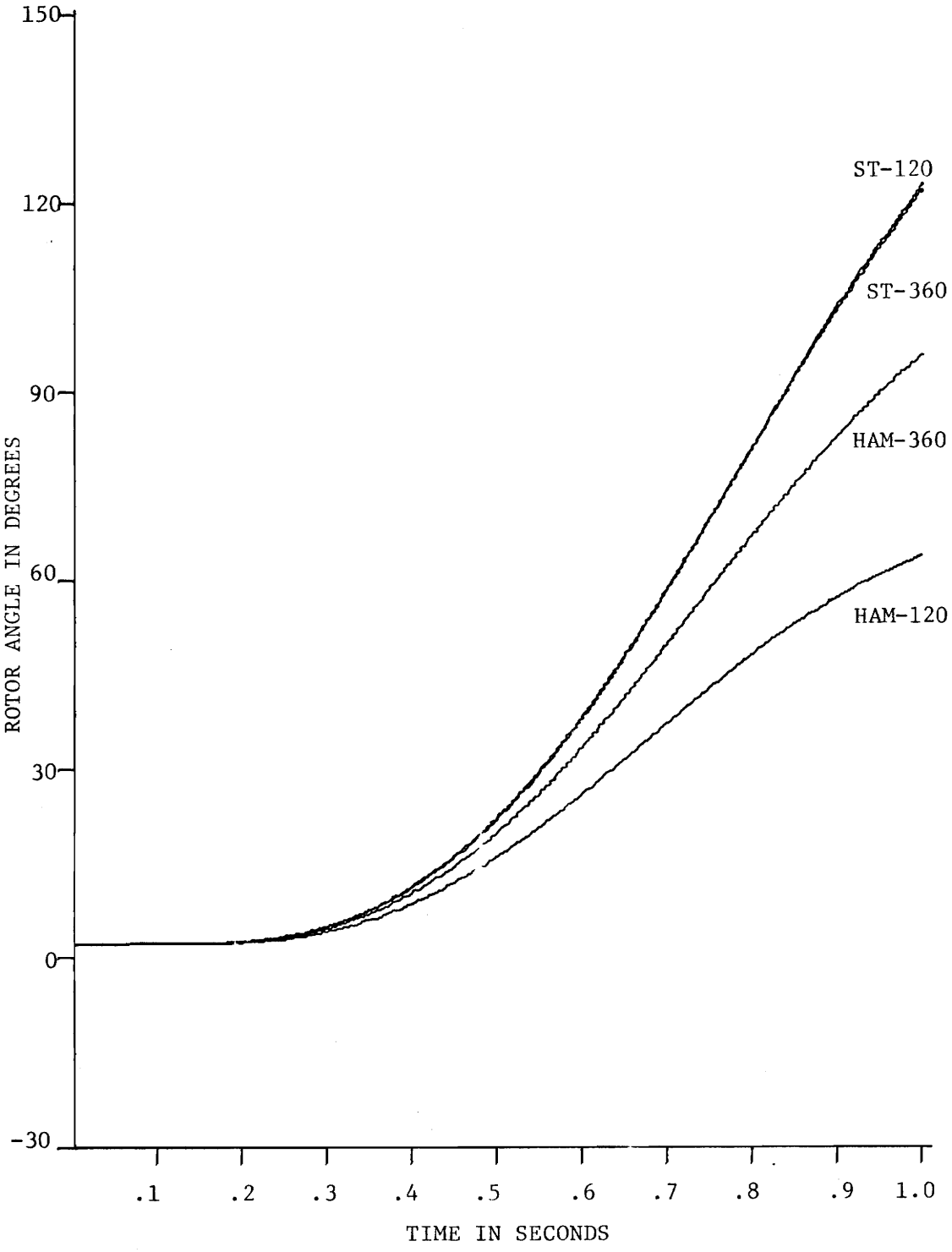

Fig. 4.2.5 Comparison of State Transition and Hamming Anderson and Fouad's 9-Bus System (δ_1)

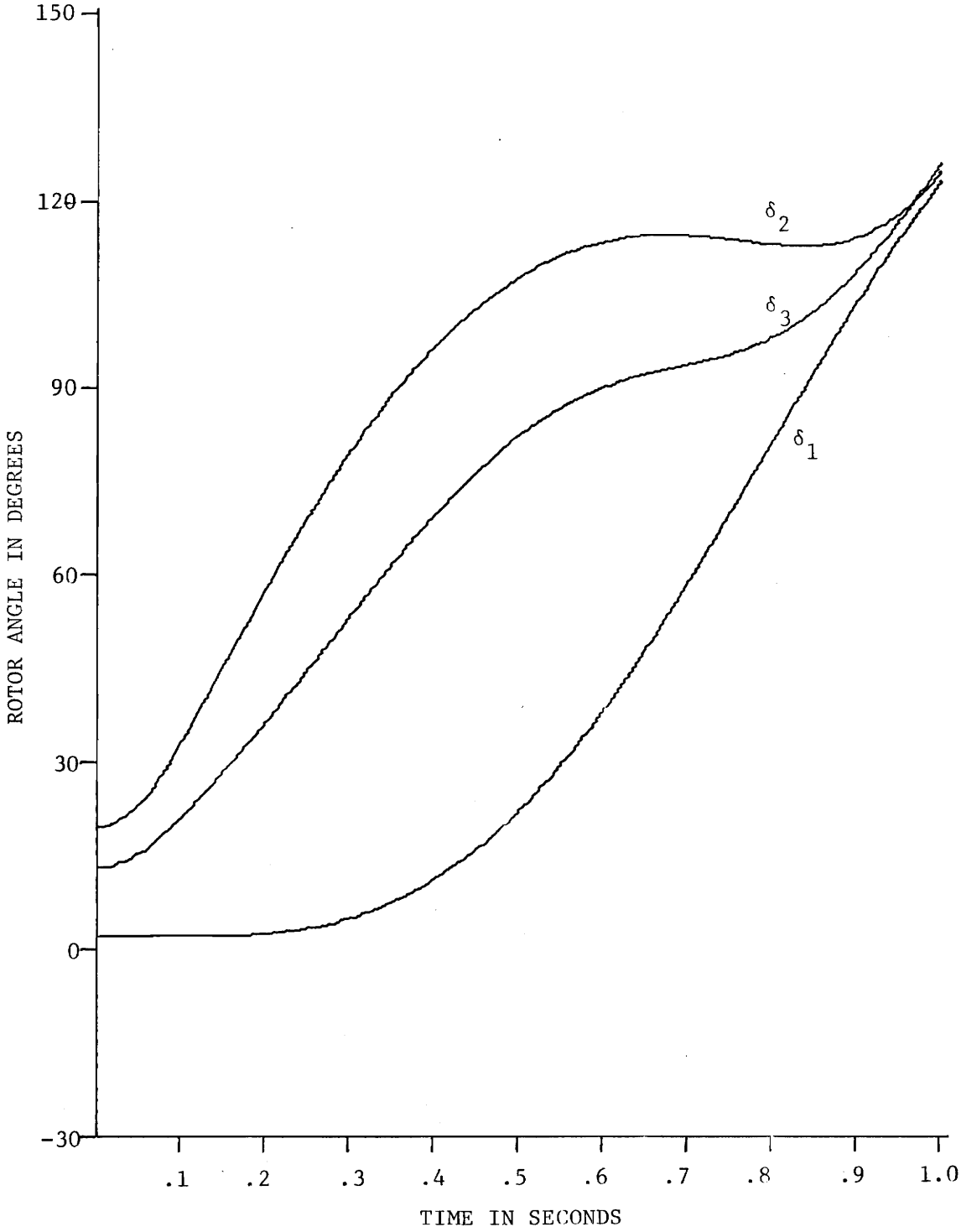

Fig. 4.2.6 Swing Curves - State Transition (h = 1/120)
Anderson and Fouad's 9-Bus System

The type of fault studied is a short near the end of line 1-6 that could be approximated as a short at bus 1. The fault was cleared after five cycles by removing line 1-6. The synchronous condensers and the static capacitor, contained in the system, were treated as constant impedance loads. Thus, the mega-var contribution of each was subtracted from the reactive demand at that bus. The synchronous condensers could have been treated as a rotating machine but, for simplicity, they were treated as loads.

Table (4.3.4) compares the compilation and execution times for each of the cases. In Tables (4.3.5)-(4.3.8), the rotor angle values are compared for the different cases for the four time intervals described in Section 4.1.

Figures 4.3.2-4.3.5 compare the swing curve of machine one for the five algorithms, using various step sizes. Fig. 4.3.6 presents the swing curves for both machines obtained using state transition (h = 1/120).

4.4 Test System III

The final system analyzed is a modified version of the IEEE fourteen-bus system. The IEEE system was modified by adding two more generators and removing the static capacitor (Fig. 4.4.1). Given system line data is presented in Table (4.4.1). The system's transformer and generator data is tabulated in Table (4.4.2) and the prefault bus data appears in Table (4.4.3).

The fault analyzed is a short on line 1-13 near bus 1. The fault was cleared after five cycles by removing line 1-13. As with the IEEE

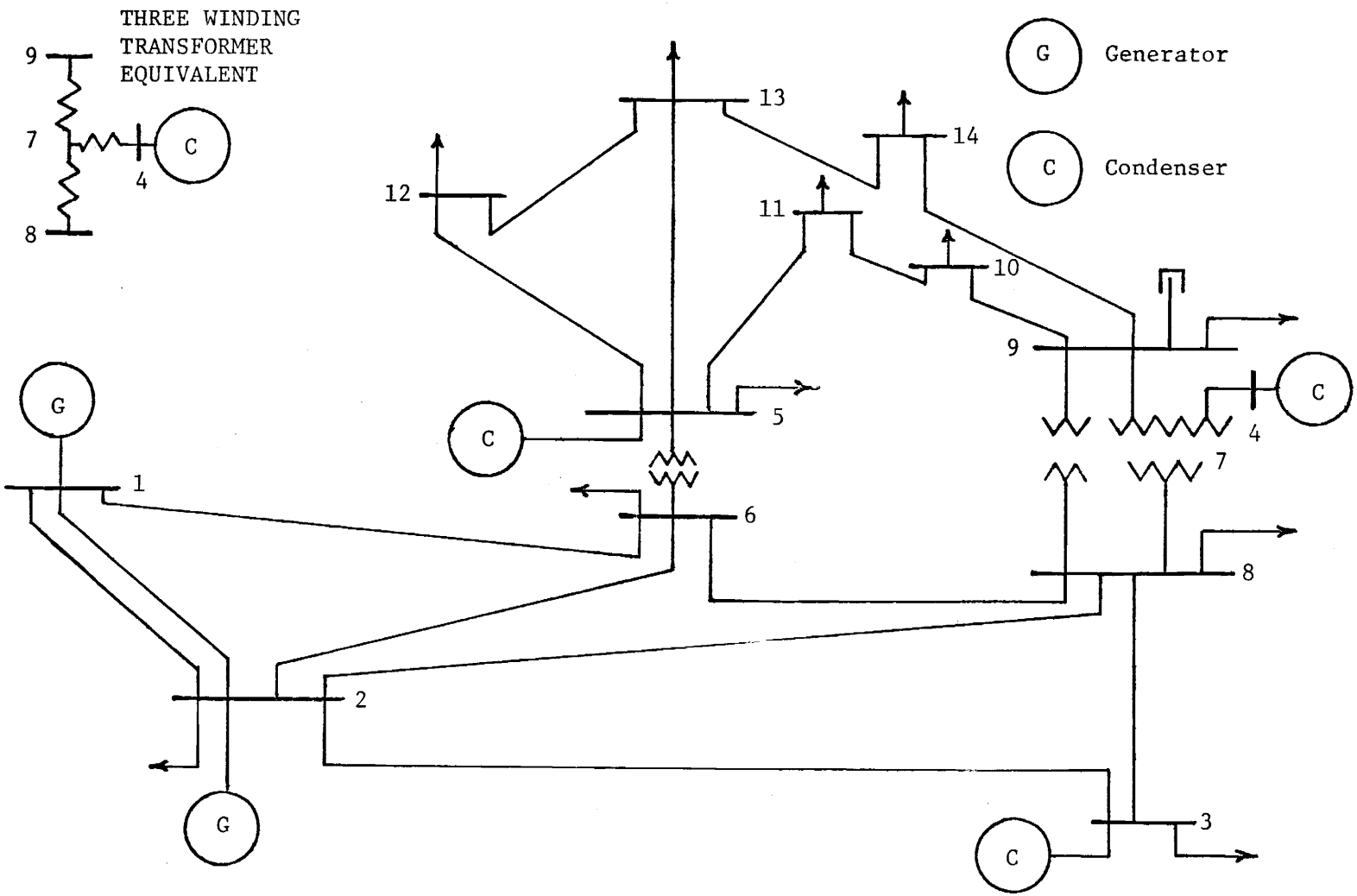

Fig. 4.3.1 Test System II

IEEE 14-Bus System

TABLE 4.3.1 IEEE 14-BUS SYSTEM LINE DATA

LINE NUMBER	STARTING BUS	ENDING BUS	RESISTANCE PER-UNIT*	REACTANCE PER-UNIT*	LINE CHARING PER-UNIT**
1	1	2	.01938	.05917	.0264
2	1	6	.05403	.22304	.0246
3	2	3	.04699	.19797	.0219
4	2	8	.05811	.17632	.0187
5	2	6	.05695	.17388	.0170
6	3	8	.06701	.17103	.0173
7	8	6	.01335	.04211	.0064
8	5	11	.09498	.19890	.0000
9	5	12	.12291	.25581	.0000
10	5	13	.06615	.13027	.0000
11	9	10	.03181	.08450	.0000
12	9	14	.12711	.27038	.0000
13	10	11	.08205	.19207	.0000
14	12	13	.22092	.19988	.0000
15	13	14	.17093	.34802	.0000

*All per-unit values are on a 100 MVA base

**Line charging is one half of total charging (B/2)

TABLE 4.3.2 IEEE 14-BUS SYSTEM TRANSFORMER AND GENERATOR DATA

TRANSFORMER NUMBER	LINE NUMBER	STARTING BUS	ENDING BUS	REACTANCE PER-UNIT*	TURNS RATIO†
1	16	8	7	.20912	.978
2	17	8	9	.55618	.969
3	18	6	5	.25202	.932
4	19	7	4	.17615	1.000
5	20	7	9	.10100	1.000

(a) TRANSFORMER DATA

GENERATOR NUMBER	INERTIA CONSTANT* MW-SEC/MVA	DAMPING COEFFICIENT MW-SEC/MVA-RAD	TRANSIENT REACTANCE PER-UNIT*
1	16.0	0.0	.2
2	2.6	0.0	.2

(b) GENERATOR DATA

*Per-unit values on a 100 MVA base

†Turns ratio is the ratio of starting bus voltage to ending bus voltage.

TABLE 4.3.3 IEEE 14-BUS SYSTEM PREFAULT BUS DATA

BUS NUMBER	GENERATOR NUMBER	BUS VOLTAGES		GENERATION		DEMAND	
		MAGNITUDE PER-UNIT	ANGLE DEGREES	REAL MW	REACTIVE MVAR	REAL MW	REACTIVE MVAR
1	1	1.060	0.00	232.4	-16.9	0.0	0.0
2	2	1.045	- 4.98	40.0	42.4	21.7	12.7
3		1.010	-12.72	0.0	23.4*	94.2	19.0
4		1.090	-13.36	0.0	17.4*	0.0	0.0
5		1.070	-14.22	0.0	12.2*	11.2	7.5
6		1.020	- 8.78			7.6	1.6
7		1.062	-13.37			0.0	0.0
8		1.019	-10.33			47.8	- 3.9
9		1.056	-14.94	-	21.2**	29.5	16.6
10		1.051	-15.10			9.0	5.8
11		1.057	-14.79			3.5	1.8
12		1.055	-15.07			6.1	1.6
13		1.050	-15.16			13.5	5.8
14		1.036	-16.04			14.9	5.0

*Condenser's contributions are treated as constant loads and subtracted from the reactive demand
**Static capacitor contribution-deducted from reactive load

TABLE 4.3.4 COMPARISON OF COMPILATION AND EXECUTION TIMES FOR THE IEEE 14-BUS SYSTEM

METHOD	STEP SIZE (1/h)	COMPILATION TIME SECONDS	EXECUTION TIME SECONDS
RUNGE-KUTTA	60	1.70	11.27
RUNGE-KUTTA	120	1.98	22.52
RUNGE-KUTTA	240	1.93	42.96
RUNGE-KUTTA	360	1.94	63.92
STATE TRANSITION	60	1.63	10.74
STATE TRANSITION	120	1.95	22.13
STATE TRANSITION	240	1.90	41.16
STATE TRANSITION	360	1.92	61.47
TRAPEZOIDAL	120	1.92	23.43
TRAPEZOIDAL	240	1.74	40.74
TRAPEZOIDAL	360	1.97	65.99
ADAMS-MOULTON	120	2.02	22.96
ADAMS-MOULTON	240	2.03	44.48
ADAMS-MOULTON	360	2.13	67.57
HAMMING	120	2.17	23.66
HAMMING	240	2.19	45.46
HAMMING	360	2.22	67.86

TABLE 4.3.5 COMPARISON OF ROTOR ANGLES (δ) FOR THE IEEE 14-BUS SYSTEM AT t = .25 SECONDS

METHOD	STEP SIZE (1/h)	δ_1 DEGREES	δ_2 DEGREES
RUNGE-KUTTA	60	47.97	16.76
RUNGE-KUTTA	120	48.35	18.24
RUNGE-KUTTA	240	48.56	19.06
RUNGE-KUTTA	360	48.63	19.35
STATE TRANSITION	60	48.84	19.51
STATE TRANSITION	120	48.80	19.76
STATE TRANSITION	240	48.79	19.86
STATE TRANSITION	360	48.79	19.89
TRAPEZOIDAL	120	48.34	18.18
TRAPEZOIDAL	240	48.56	19.04
TRAPEZOIDAL	360	48.63	19.34
ADAMS-MOULTON	120	48.07	16.97
ADAMS-MOULTON	240	48.38	18.29
ADAMS-MOULTON	360	48.50	18.80
HAMMING	120	48.07	16.96
HAMMING	240	48.38	18.29
HAMMING	360	48.50	18.80

TABLE 4.3.6 COMPARISON OF ROTOR ANGLES (δ) FOR THE IEEE 14-BUS SYSTEM AT t = .50 SECONDS

METHOD	STEP SIZE (1/h)	δ_1 DEGREES	δ_2 DEGREES
RUNGE-KUTTA	60	74.46	47.99
RUNGE-KUTTA	120	78.38	51.88
RUNGE-KUTTA	240	80.59	54.07
RUNGE-KUTTA	360	81.37	54.84
STATE TRANSITION	60	83.10	56.47
STATE TRANSITION	120	83.06	56.36
STATE TRANSITION	240	83.03	56.39
STATE TRANSITION	360	83.02	56.41
TRAPEZOIDAL	120	78.34	51.94
TRAPEZOIDAL	240	80.58	54.09
TRAPEZOIDAL	360	81.36	54.85
ADAMS-MOULTON	120	74.74	48.24
ADAMS-MOULTON	240	78.45	51.95
ADAMS-MOULTON	360	79.87	53.35
HAMMING	120	74.73	48.23
HAMMING	240	78.45	51.94
HAMMING	360	79.86	53.35

TABLE 4.3.7 COMPARISON OF ROTOR ANGLES (δ) FOR THE IEEE 14-BUS SYSTEM AT t = .75 SECONDS

METHOD	STEP SIZE (1/h)	δ_1 DEGREES	δ_2 DEGREES
RUNGE-KUTTA	60	100.71	75.70
RUNGE-KUTTA	120	110.10	86.81
RUNGE-KUTTA	240	115.54	93.44
RUNGE-KUTTA	360	117.48	95.83
STATE TRANSITION	60	121.77	103.43
STATE TRANSITION	120	121.65	102.27
STATE TRANSITION	240	121.61	101.60
STATE TRANSITION	360	121.60	101.38
TRAPEZOIDAL	120	110.06	86.65
TRAPEZOIDAL	240	115.53	93.39
TRAPEZOIDAL	360	117.48	95.81
ADAMS-MOULTON	120	101.12	76.07
ADAMS-MOULTON	240	110.20	86.90
ADAMS-MOULTON	360	113.71	91.17
HAMMING	120	101.10	76.05
HAMMING	240	110.20	86.90
HAMMING	360	113.70	91.17

TABLE 4.3.8 COMPARISON OF ROTOR ANGLES (δ) FOR THE IEEE 14-BUS SYSTEM AT t = 1.00 SECONDS

METHOD	STEP SIZE (1/h)	δ_1 DEGREES	δ_2 DEGREES
RUNGE-KUTTA	60	126.33	96.06
RUNGE-KUTTA	120	144.02	112.33
RUNGE-KUTTA	240	154.78	122.22
RUNGE-KUTTA	360	158.71	125.84
STATE TRANSITION	60	169.46	127.86
STATE TRANSITION	120	168.15	131.02
STATE TRANSITION	240	167.62	132.41
STATE TRANSITION	360	167.45	132.83
TRAPEZOIDAL	120	143.95	112.37
TRAPEZOIDAL	240	154.76	122.23
TRAPEZOIDAL	360	158.70	125.84
ADAMS-MOULTON	120	126.82	96.61
ADAMS-MOULTON	240	144.15	112.48
ADAMS-MOULTON	360	151.08	118.84
HAMMING	120	126.80	96.59
HAMMING	240	144.13	112.46
HAMMING	360	151.05	118.81

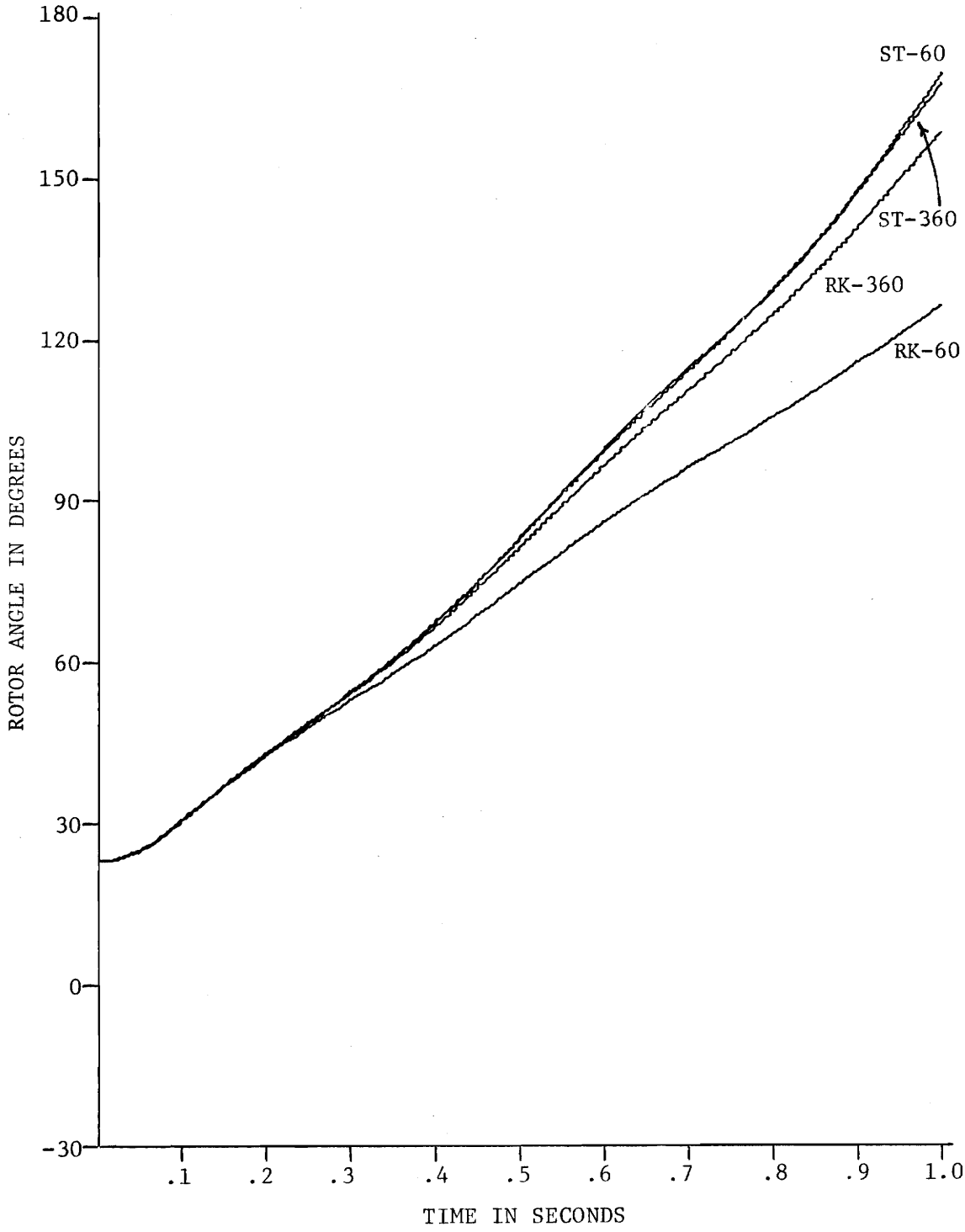

Fig. 4.3.2 Comparison of State Transition and Runge-Kutta IEEE 14-Bus System (δ_1)

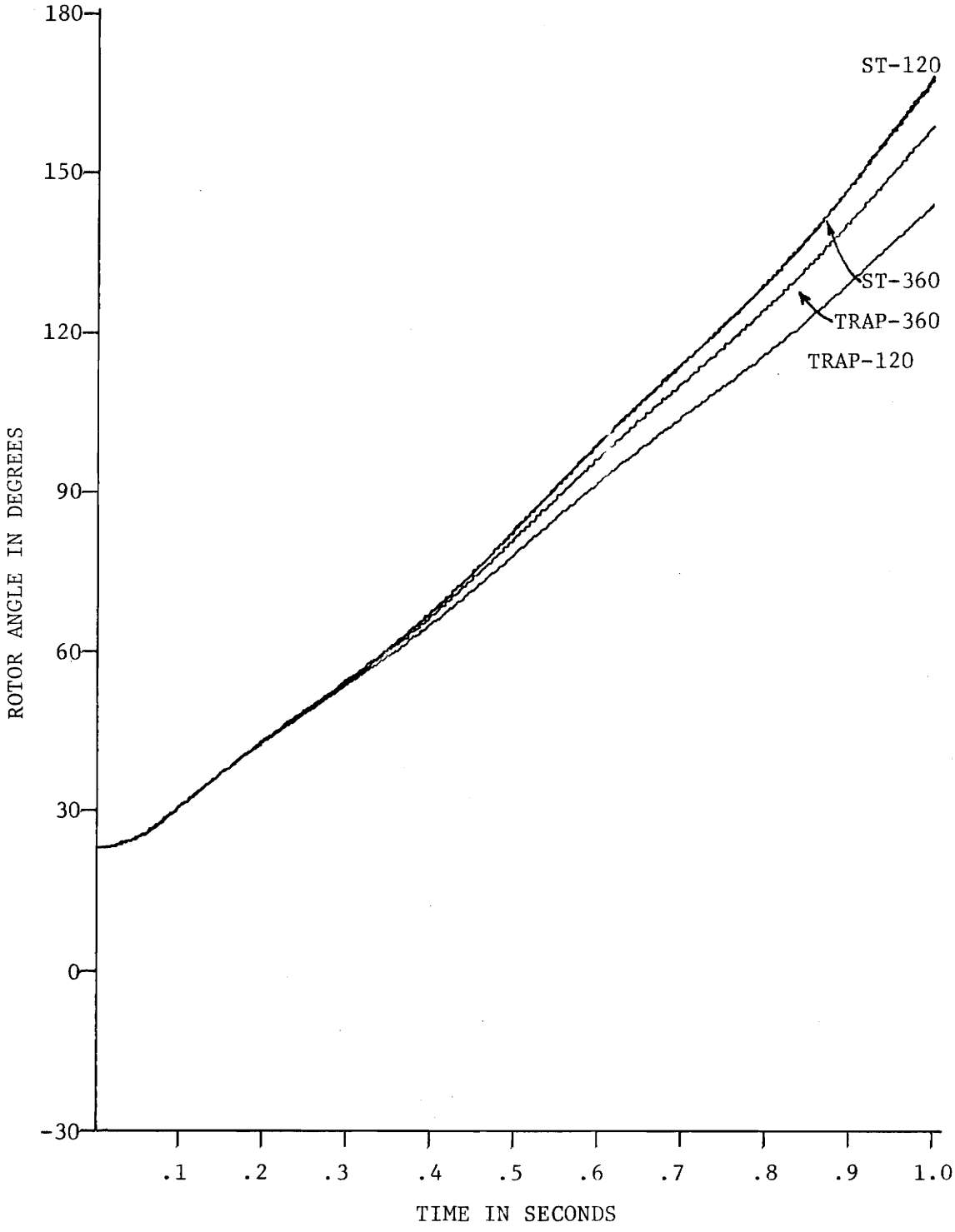

Fig. 4.3.3 Comparison of State Transition and the Trapezoidal Rule IEEE 14-Bus System (δ_1)

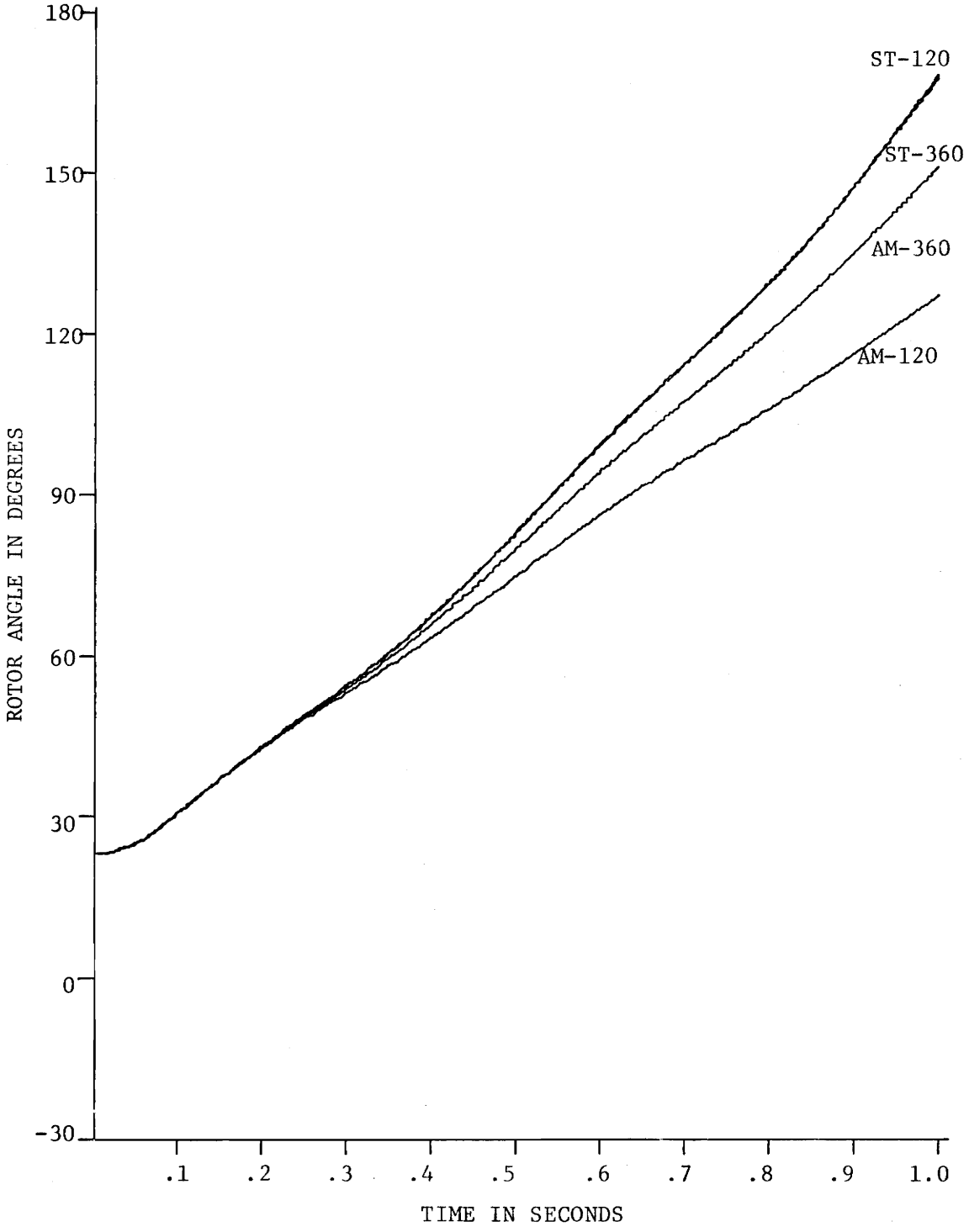

Fig. 4.3.4 Comparison of State Transition and Adams-Moulton IEEE 14-Bus System (δ_1)

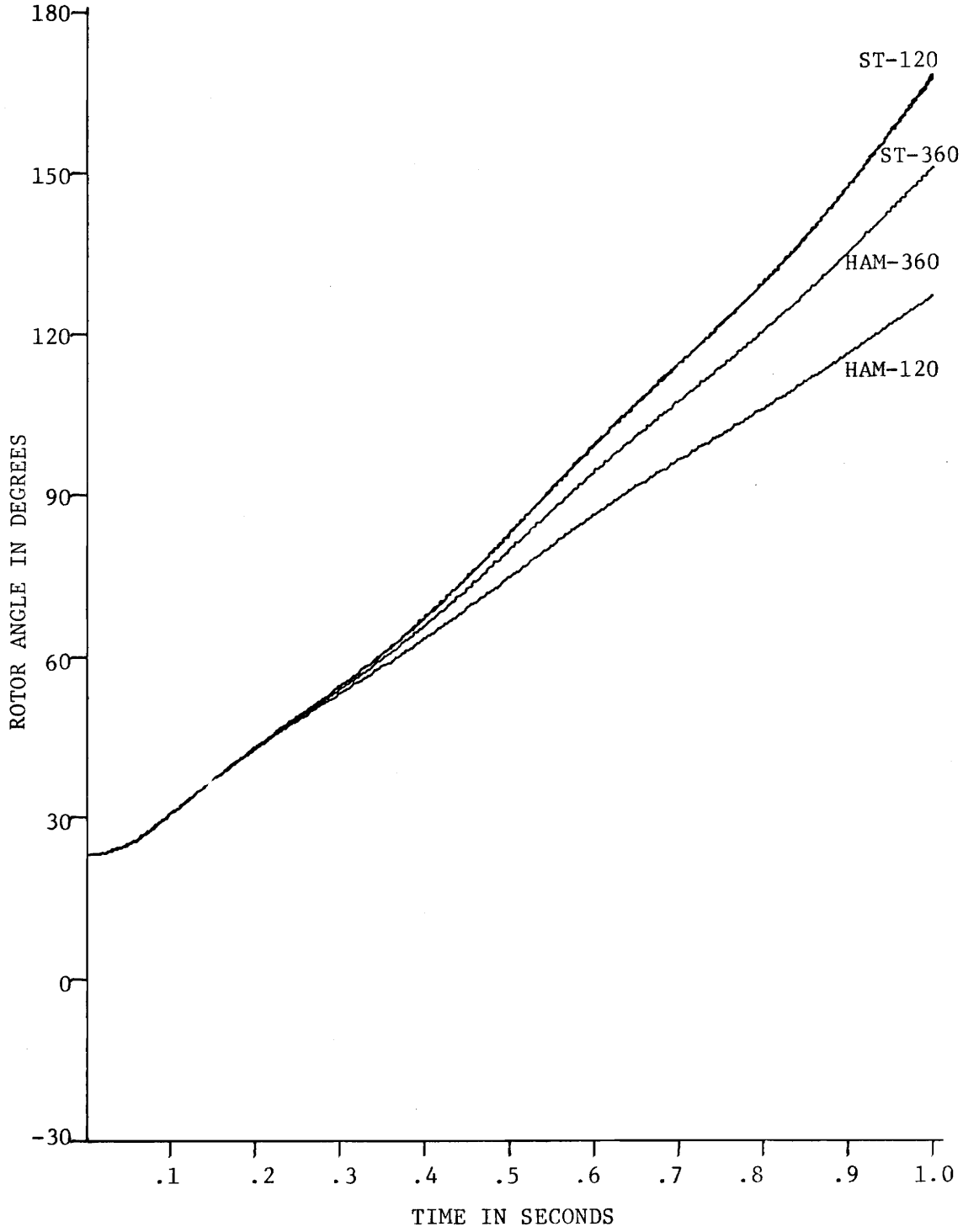

Fig. 4.3.5 Comparison of State Transition and Hamming IEEE 14-Bus System (δ_1)

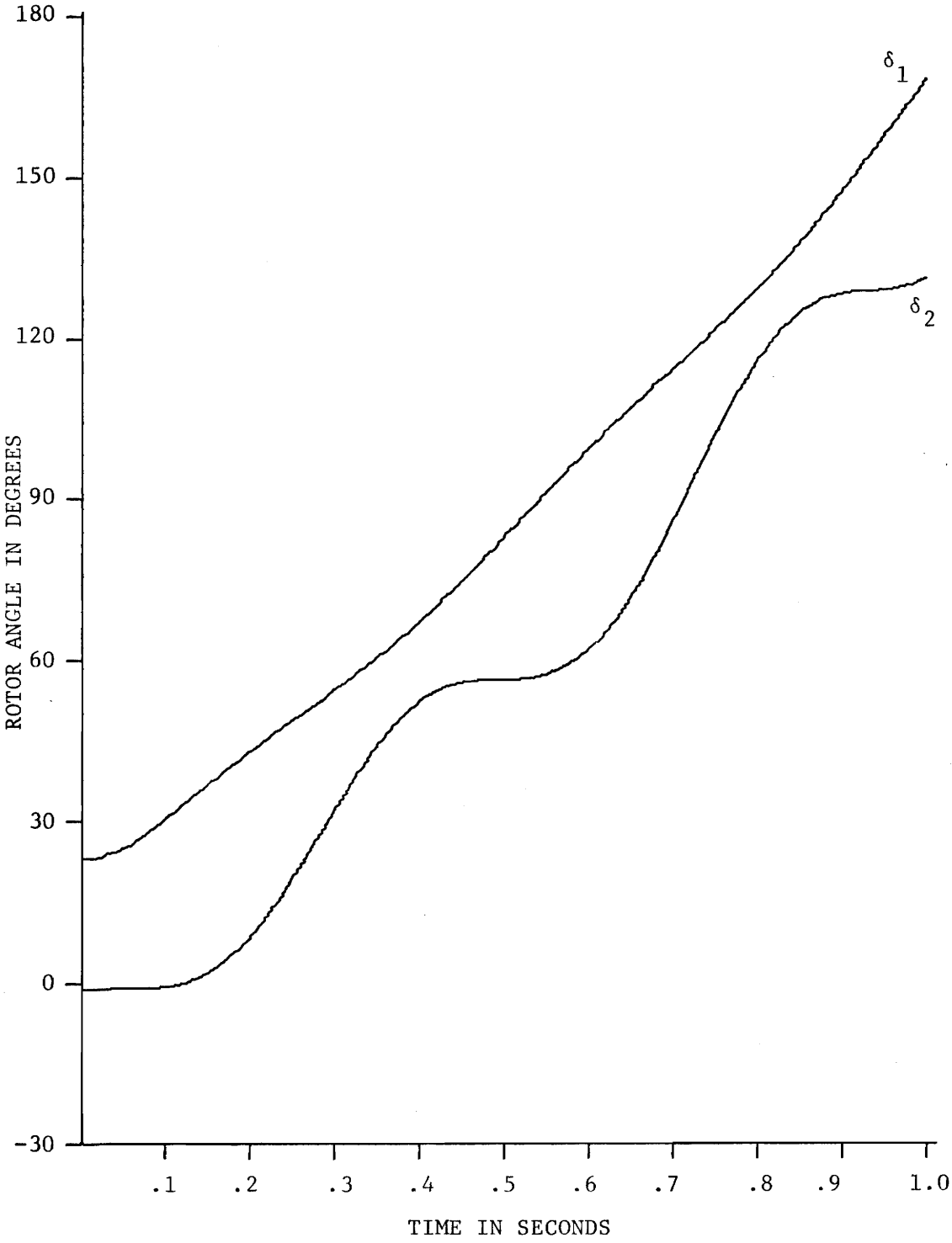

Fig. 4.3.6 Swing Curves - State Transition (h = 1/120)
IEEE 14-Bus System

system, the synchronous condensers of the modified system were treated as constant impedance loads.

The compilation and execution times for each case are compared in Table (4.4.4). The rotor angle values obtained from the different cases are compared for the four time intervals in Tables (4.4.5)-(4.4.8).

Plots, comparing the swing curve of machine one, for different cases, are presented in Figs. 4.4.2-4.4.5. The swing curves for all machines, obtained using state transition (h = 1/120), are presented in Fig. 4.4.6.

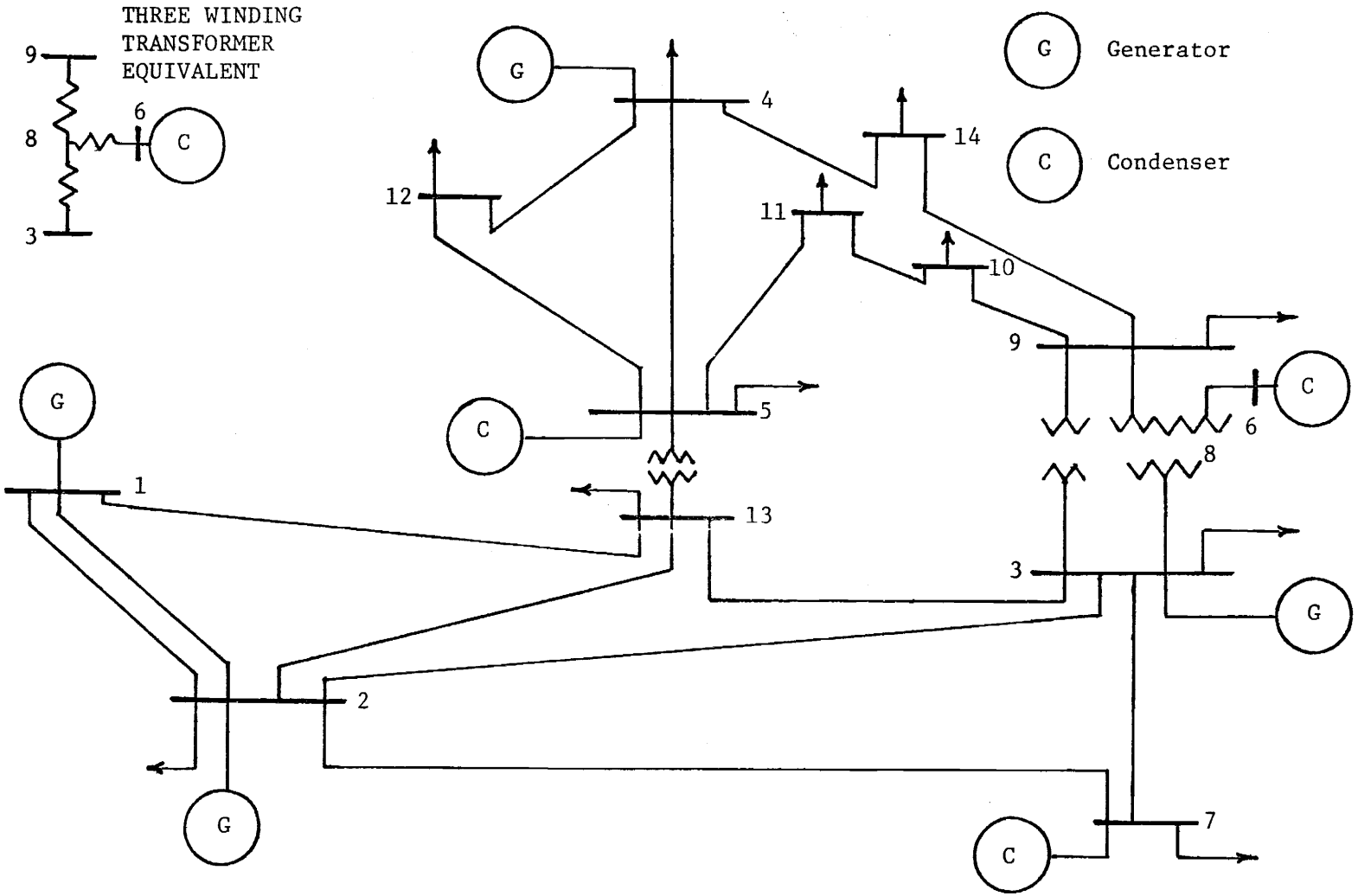

Fig. 4.4.1 Test System III
Modified IEEE 14-Bus System

TABLE 4.4.1 MODIFIED IEEE 14-BUS SYSTEM
LINE DATA

LINE NUMBER	STARTING BUS	ENDING BUS	RESISTANCE PER-UNIT*	REACTANCE PER-UNIT*	LINE CHARGING PER-UNIT**
1	1	2	.01938	.05917	.0264
2	1	13	.05403	.22304	.0246
3	2	7	.04699	.19797	.0219
4	2	3	.05811	.17632	.0187
5	2	13	.05695	.17388	.0170
6	7	3	.06701	.17103	.0173
7	3	13	.01335	.04211	.0064
8	5	11	.09498	.19890	.0000
9	5	12	.12291	.25581	.0000
10	5	4	.06615	.13027	.0000
11	9	10	.03181	.08450	.0000
12	9	14	.12711	.27038	.0000
13	10	11	.08205	.19207	.0000
14	12	4	.22092	.19988	.0000
15	4	14	.17093	.34802	.0000

* All per-unit values are on a 100 MVA base

** Line charging is one half of total charging (B/2)

TABLE 4.4.2 MODIFIED IEEE 14-BUS SYSTEM
TRANSFORMER & GENERATOR DATA

TRANSFORMER NUMBER	LINE NUMBER	STARTING BUS	ENDING BUS	REACTANCE PER-UNIT*	TURNS RATIO†
1	16	3	8	.20912	.978
2	17	3	9	.55618	.969
3	18	13	5	.25202	.932
4	19	8	6	.17615	1.000
5	20	8	9	.11001	1.000

(a) TRANSFORMER DATA

GENERATOR NUMBER	INERTIA CONSTANT* MW-SEC/MVA	DAMPING COEFFICIENT MW-SEC/MVA-RAD	TRANSIENT REACTANCE PER-UNIT*
1	16.00	0.0	.2
2	3.00	0.0	.2
3	2.00	0.0	.2
4	2.50	0.0	.2

(b) GENERATOR DATA

*Per-Unit values on a 100 MVA base

†Turns ratio is the ratio of starting bus voltage to ending bus voltage.

TABLE 4.4.3 MODIFIED IEEE 14-BUS SYSTEM
PREFAULT BUS DATA

BUS NUMBER	GENERATOR NUMBER	BUS VOLTAGES		GENERATION		DEMAND	
		MAGNITUDE PER-UNIT	ANGLE DEGREES	REAL MW	REACTIVE MVAR	REAL MW	REACTIVE MVAR
1	1	1.0600	0.00	145.91	-4.22	0.00	0.00
2	2	1.0450	-3.11	40.00	19.35	21.70	12.70
3	3	1.0306	-6.21	40.00	10.00	47.80	-3.90
4	4	1.0738	-7.01	40.00	10.00	13.50	5.80
5		1.0700	-7.45	0.00	-.50*	11.20	7.50
6		1.0900	-8.25	0.00	20.12*	0.00	0.00
7		1.0100	-9.54	0.00	17.04*	94.20	19.00
8		1.0575	-8.25			0.00	0.00
9		1.0397	-9.34			29.50	16.60
10		1.0372	-9.29			9.00	5.80
11		1.0495	-8.50			3.50	1.80
12		1.0642	-7.51			6.10	1.60
13		1.0310	-5.19			7.60	1.60
14		1.0361	-9.30			14.90	5.00

* Condenser's contributions are treated as constant loads and subtracted from the reactive demand

TABLE 4.4.4 COMPARISON OF COMPILATION AND EXECUTION TIMES FOR THE MODIFIED IEEE 14-BUS SYSTEM

METHOD	STEP SIZE (1/h)	COMPILATION TIME SECONDS	EXECUTION TIME SECONDS
RUNGE-KUTTA	60	2.02	13.64
RUNGE-KUTTA	120	1.91	24.39
RUNGE-KUTTA	240	1.92	46.30
RUNGE-KUTTA	360	2.00	71.71
STATE TRANSITION	60	1.88	12.40
STATE TRANSITION	120	1.86	21.92
STATE TRANSITION	360	1.94	63.33
TRAPEZOIDAL	120	1.91	27.57
TRAPEZOIDAL	240	1.95	50.08
TRAPEZOIDAL	360	1.97	74.63
ADAMS-MOULTON	120	2.10	25.44
ADAMS-MOULTON	240	2.10	48.85
ADAMS-MOULTON	360	2.04	71.56
HAMMING	60	2.17	15.12
HAMMING	120	2.13	27.17
HAMMING	240	2.11	52.51
HAMMING	360	2.10	76.75

TABLE 4.4.5 COMPARISON OF ROTOR ANGLES (δ) FOR THE MODIFIED IEEE 14-BUS SYSTEM AT t = .25 SECONDS

METHOD	STEP SIZE (1/h)	δ_1 DEGREES	δ_2 DEGREES	δ_3 DEGREES	δ_4 DEGREES
RUNGE-KUTTA	60	27.38	1.79	-2.83	-10.19
RUNGE-KUTTA	120	27.38	1.58	-3.13	-11.02
RUNGE-KUTTA	240	27.37	1.44	-3.31	-11.50
RUNGE-KUTTA	360	27.37	1.38	-3.38	-11.68
STATE TRANSITION	60	27.62	.79	-3.77	-13.01
STATE TRANSITION	120	27.48	1.03	-3.62	-12.52
STATE TRANSITION	360	27.40	1.19	-3.55	-12.20
TRAPEZOIDAL	120	27.38	1.57	-3.16	-11.03
TRAPEZOIDAL	240	27.37	1.44	-3.32	-11.51
TRAPEZOIDAL	360	27.37	1.38	-3.38	-11.68
ADAMS-MOULTON	120	27.36	1.63	-3.04	-10.51
ADAMS-MOULTON	240	27.37	1.53	-3.19	-11.11
ADAMS-MOULTON	360	27.37	1.46	-3.28	-11.38
HAMMING	60	27.32	1.62	-3.05	-9.93
HAMMING	120	27.36	1.64	-3.04	-10.50
HAMMING	240	27.37	1.53	-3.19	-11.11
HAMMING	360	27.37	1.46	-3.28	-11.38

TABLE 4.4.6 COMPARISON OF ROTOR ANGLES (δ) FOR THE MODIFIED IEEE 14-BUS SYSTEM AT t = .50 SECONDS

METHOD	STEP SIZE (1/h)	δ_1 DEGREES	δ_2 DEGREES	δ_3 DEGREES	δ_4 DEGREES
RUNGE-KUTTA	60	27.46	18.95	13.99	17.84
RUNGE-KUTTA	120	28.16	21.26	16.53	22.00
RUNGE-KUTTA	240	28.53	22.63	18.06	24.49
RUNGE-KUTTA	360	28.66	23.12	18.62	25.39
STATE TRANSITION	60	28.27	25.59	19.38	30.49
STATE TRANSITION	120	28.60	24.80	19.75	28.84
STATE TRANSITION	360	28.82	24.37	19.82	27.81
TRAPEZOIDAL	120	28.13	21.24	16.46	21.95
TRAPEZOIDAL	240	28.52	22.62	18.04	24.47
TRAPEZOIDAL	360	28.66	23.12	18.61	25.38
ADAMS-MOULTON	120	27.21	18.84	13.84	17.78
ADAMS-MOULTON	240	28.08	21.22	16.47	21.98
ADAMS-MOULTON	360	28.37	22.14	17.50	23.61
HAMMING	60	25.60	15.31	10.01	11.72
HAMMING	120	27.21	18.85	13.84	17.78
HAMMING	240	28.08	21.22	16.48	21.98
HAMMING	360	28.37	22.14	17.50	23.61

TABLE 4.4.7 COMPARISON OF ROTOR ANGLES (δ) FOR THE MODIFIED IEEE 14-BUS SYSTEM AT t = .75 SECONDS

METHOD	STEP SIZE (1/h)	δ_1 DEGREES	δ_2 DEGREES	δ_3 DEGREES	δ_4 DEGREES
RUNGE-KUTTA	60	35.47	18.55	11.39	8.81
RUNGE-KUTTA	120	40.10	22.05	14.24	10.49
RUNGE-KUTTA	240	42.98	24.30	16.09	11.60
RUNGE-KUTTA	360	44.05	25.15	16.78	12.03
STATE TRANSITION	60	47.15	28.32	15.43	10.01
STATE TRANSITION	120	46.76	27.52	16.92	11.54
STATE TRANSITION	360	46.50	27.14	17.88	12.51
TRAPEZOIDAL	120	40.03	22.06	14.32	10.55
TRAPEZOIDAL	240	42.96	24.30	16.11	11.62
TRAPEZOIDAL	360	44.04	25.15	16.79	12.04
ADAMS-MOULTON	120	35.18	18.24	11.10	8.55
ADAMS-MOULTON	240	40.00	21.95	14.15	10.40
ADAMS-MOULTON	360	41.92	23.46	15.39	11.16
HAMMING	60	28.51	13.20	6.99	5.98
HAMMING	120	35.19	18.24	11.11	8.56
HAMMING	240	40.00	21.95	14.15	10.41
HAMMING	360	41.92	23.46	15.39	11.16

TABLE 4.4.8 COMPARISON OF ROTOR ANGLES (δ) FOR THE MODIFIED IEEE 14-BUS SYSTEM AT t = 1.00 SECONDS

METHOD	STEP SIZE (1/h)	δ_1 DEGREES	δ_2 DEGREES	δ_3 DEGREES	δ_4 DEGREES
RUNGE-KUTTA	60	39.49	22.46	19.16	17.36
RUNGE-KUTTA	120	45.98	28.79	26.07	24.41
RUNGE-KUTTA	240	50.27	33.02	30.69	29.14
RUNGE-KUTTA	360	51.90	34.63	32.46	30.95
STATE TRANSITION	60	56.62	33.72	40.37	34.62
STATE TRANSITION	120	55.94	36.79	37.57	35.09
STATE TRANSITION	360	55.65	37.87	36.66	35.06
TRAPEZOIDAL	120	45.99	28.63	25.99	24.21
TRAPEZOIDAL	240	50.27	32.97	30.66	29.08
TRAPEZOIDAL	360	51.91	34.61	32.44	30.92
ADAMS-MOULTON	120	39.20	22.09	18.82	16.90
ADAMS-MOULTON	240	45.87	28.66	25.94	24.24
ADAMS-MOULTON	360	48.69	31.44	28.98	27.37
HAMMING	60	30.95	14.13	10.24	8.16
HAMMING	120	39.21	22.10	18.83	16.91
HAMMING	240	45.87	28.66	25.94	24.24
HAMMING	360	48.69	31.44	28.98	27.37

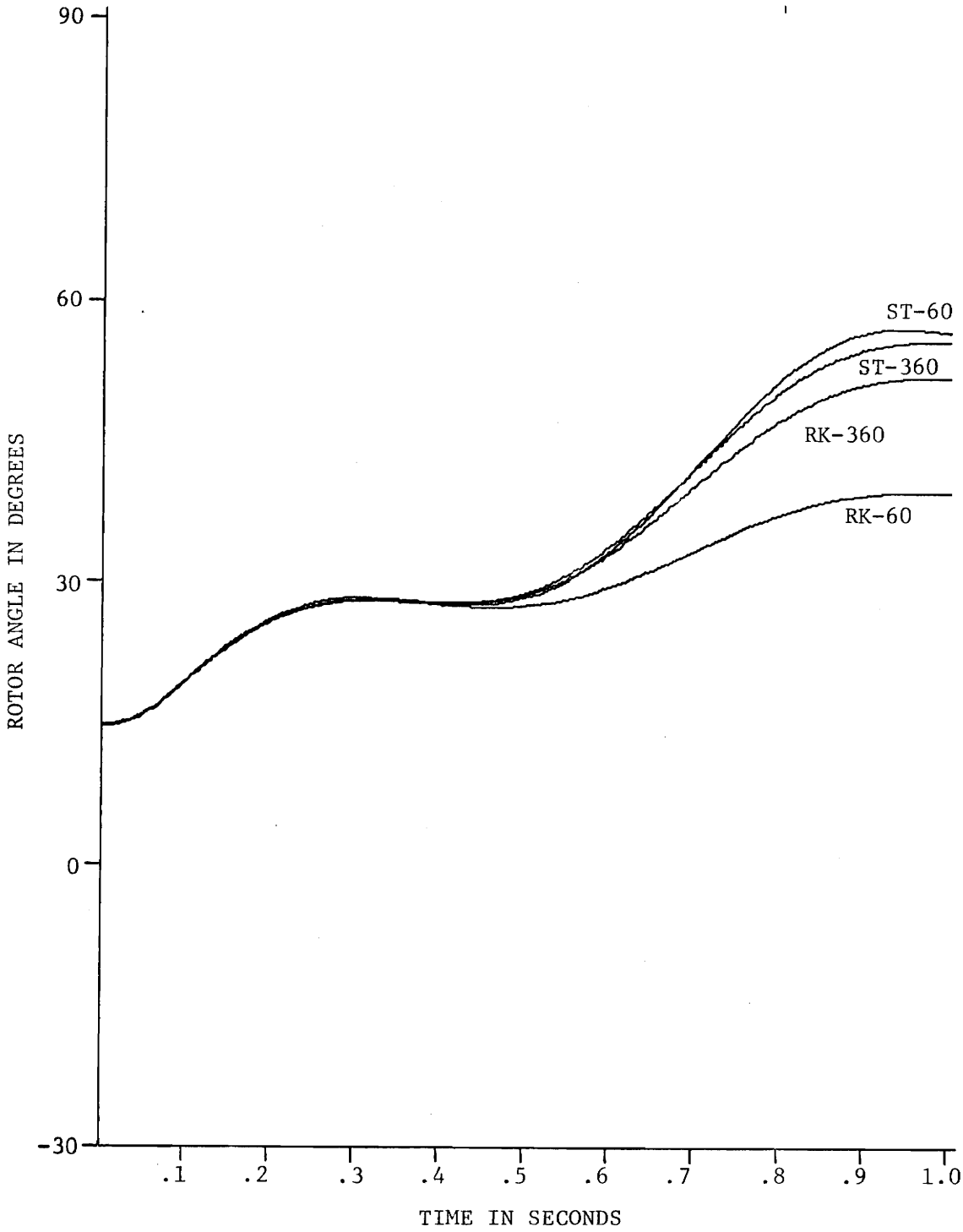

Fig. 4.4.2 Comparison of State Transition and Runge-Kutta Modified IEEE 14-Bus System (δ_1)

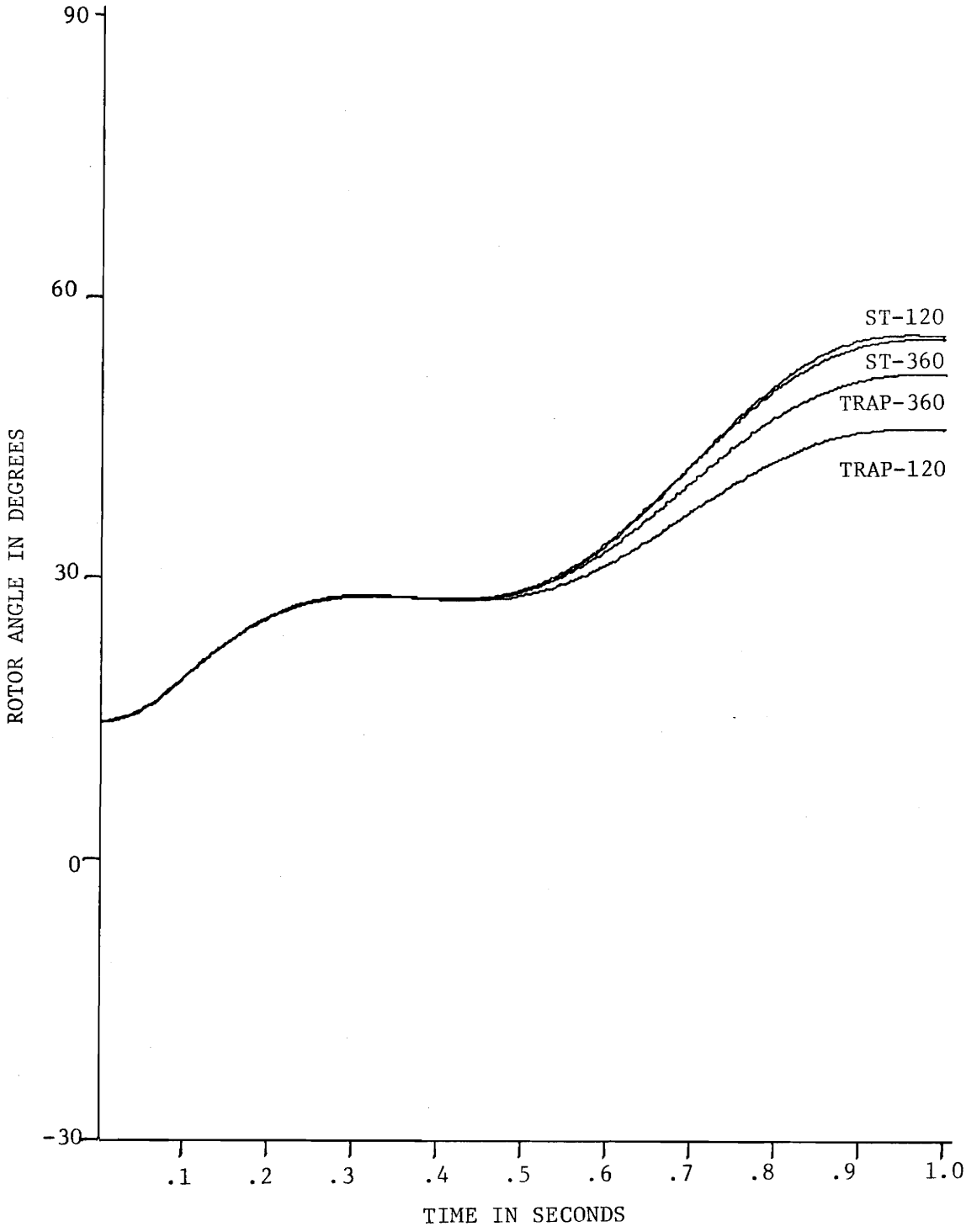

Fig. 4.4.3 Comparison of State Transition and the Trapezoidal Rule Modified IEEE 14-Bus System (δ_1)

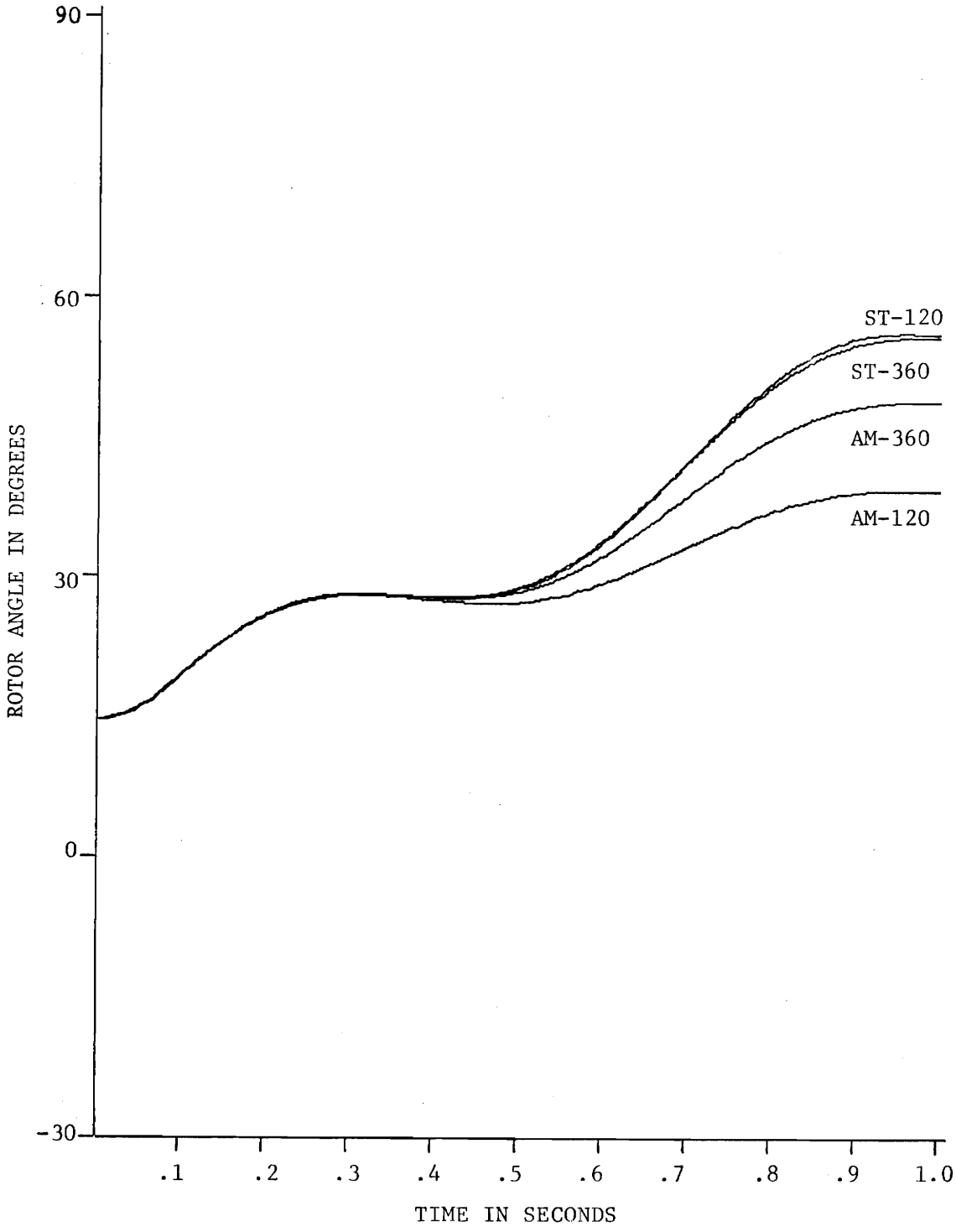

Fig. 4.4.4 Comparison of State Transition and Adams-Moulton Modified IEEE 14-Bus System (δ_1)

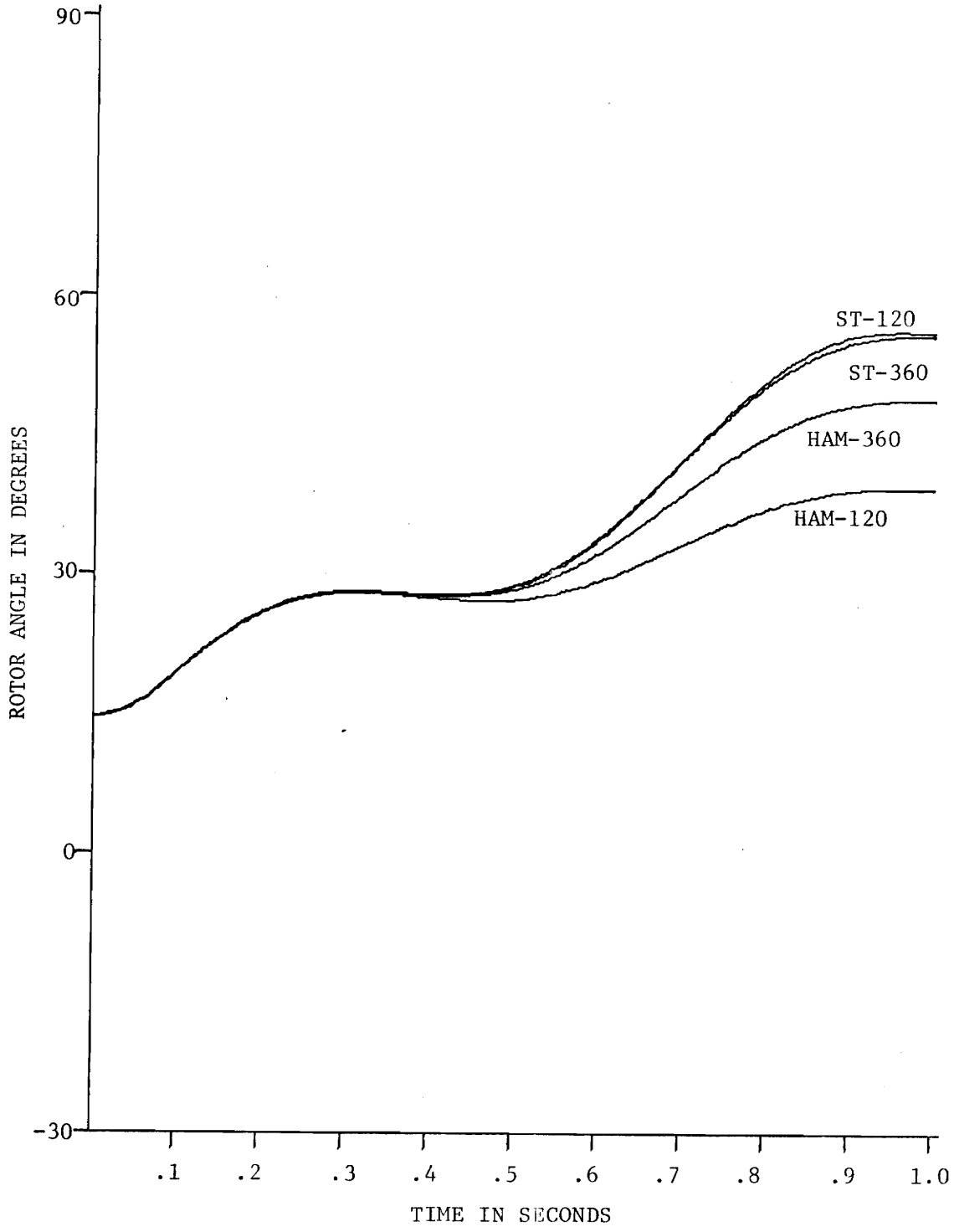

Fig. 4.4.5 Comparison of State Transition and Hamming Modified IEEE 14-Bus System (δ_1)

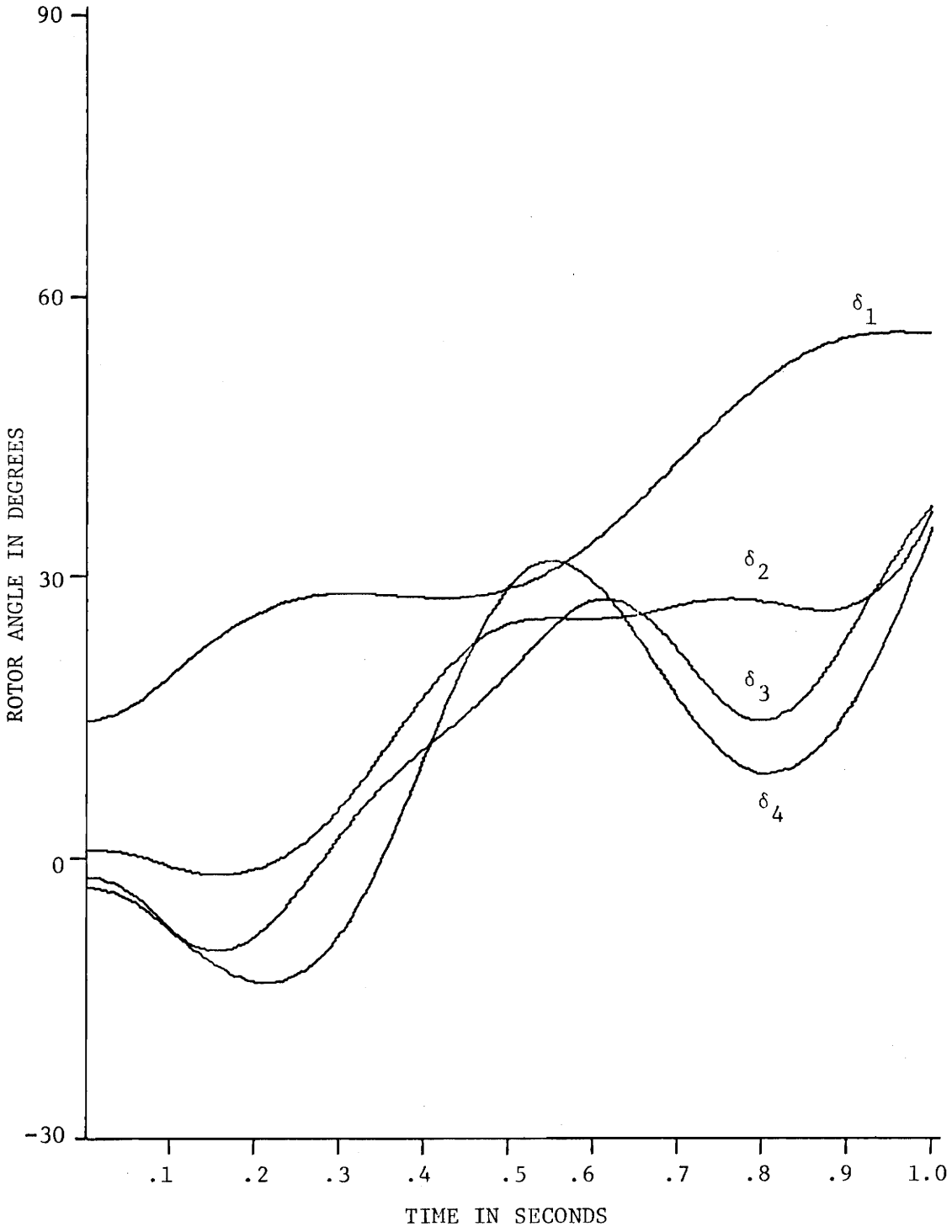

Fig. 4.4.6 Swing Curves - State Transition (h = 1/120)
Modified IEEE 14-Bus System

V. CONCLUSION

5.1 Introduction

In this, the closing chapter, the results presented in the preceding chapter will be discussed and compared. Remarks concerning the relative accuracy, ease of programming and speed of solution time of each algorithm will be made. Recommendations for areas of further research and study are contained in the final section.

5.2 Comparison of Results

Since there is no benchmark solution, i.e. exact solution, to compare the methods to, conclusions must be drawn on the merits of the results obtained. By close examination of the tables, comparing the rotor angle values, and the graphs, comparing the various cases, obvious conclusions can be drawn.

In terms of relative accuracy, state transition, by far, produces the best results. Using state transition with step sizes from 1/60 to 1/360, the rotor angle values varied by no more than five degrees for any of the three systems. For the other four methods, the values varied by as much as twenty-five or thirty degrees and, in some cases, more. This consistent accuracy is well illustrated by the graphs in the preceding chapter. This accuracy is reasonable when it is considered that the state transition solution is a closed form solution (the other methods are approximate solution methods). The only approximation made, when using state transition, is that the accelerating power remains constant for the interval in question. Since the accelerating power is a function of the sine and cosine of the rotor angles, it is understandable that,

for time steps of the order of 1/60 or smaller, the power will not vary much because the rotor angles themselves do not vary much. Thus the clamping of the power produces a very accurate approximation.

For the purpose of discussing the relative accuracy of the other methods, we will use state transition (h = 1/120) as the standard since the results produced by the other algorithms, as the step size was reduced, approached the results obtained using state transition. The trapezoidal rule and fourth-order Runge-Kutta consistently produced results that were nearly identical (less than one degree difference) for the same step size. These two methods, however, did not produce results as accurate as state transition produced, even for a step size as small as 1/360.

Both the predictor-corrector methods, Adams-Moulton and Hamming, produced nearly identical results (less than one degree difference) for the same step size. The results produced by the predictor-corrector methods, for a given step size, were comparable to those produced by Runge-Kutta and the trapezoidal rule using a step size twice as large.

For comparing the solution times of each algorithm, the total execution time, for the solution of the stability problem by the IBM 370 computer, was used. Since a common main program was used to call a subroutine for a particular algorithm, any difference in the total execution time, for a particular system, must be due to the numerical algorithm.

State transition was consistently the fastest method for the three systems analyzed. The execution times for state transition for the nine-bus system and the modified IEEE system, were approximately ten percent

faster than those for Runge-Kutta. (Runge-Kutta produced the second fastest times in nearly all cases.) There was only a slight difference between the solution times of the two methods for the IEEE system. Since the IEEE system contained fourteen buses and only two generators, it is possible that the solution time of the differential equations was insignificant when compared to the total solution time.

In terms of solution time for the other three methods, no specific trend was observed. For some cases one method was faster, while in other cases, another method was faster. For the most part, the times were nearly the same for all three algorithms.

In regard to ease of programming, state transition was the simplest method to implement. It required the least number of steps (using Fortran) and the least amount of logic. Runge-Kutta and the trapezoidal rule were of comparable difficulty to program and were second to state transition. The difficulty encountered with Runge-Kutta was that four function evaluations ($\dot{\underline{x}}$) were required for each time step. The predictor-corrector methods were the most difficult to program. Since these methods are not self-starting, they required a built-in Runge-Kutta routine to start them whenever a system configuration change occurred. This Runge-Kutta routine and its associated logic presented the difficulty in programming the predictor-corrector methods.

In conclusion, a comparison of the advantages and disadvantages of the five algorithms, as applied to the second-order swing equation, is presented.

The advantages of state transition are as follows:

(1) The method utilizes a closed form solution with the approximation that the accelerating power is clamped. Thus, highly accurate results are obtained.

(2) A fast solution is produced since the $\underline{A}$ and $\underline{B}$ matrices are constant and, thus, the solution is simply a matrix multiplication operation.

(3) The method is easy to implement for the reasons stated above.

There were no disadvantages encountered with the state transition algorithm.

The advantages of fourth-order Runge-Kutta are:

(1) The method is self-starting and, thus, relatively easy to program.

(2) Good accuracy is produced for a small "enough" time step.

(3) A relatively fast solution time is produced.

The disadvantages are:

(1) Four function evaluations are required per step.

(2) The method is subject to numerical instability [6].

(3) There is no method of error estimate at a given point.

The trapezoidal rule has the following advantages:

(1) The method is self-starting and relatively easy to program.

(2) The method is numerically stable [6].

(3) The results are relatively accurate even though the truncation error is of the order (h^3).

The disadvantage is that the method is implicit and requires iterations for the solution at every step. These iterations, inhibit the speed of solution time.

The Adams-Moulton has the following advantages:

(1) Error estimate is available at every step.

(2) The truncation error is of the order of (h^5). This means the accuracy should be high but Adams-Moulton and Hamming produced the least accurate results.

The disadvantages are:

(1) The method is not self-starting and, thus, requires an additional routine to provide starting values at every discontinuity.

(2) The corrector is implicit. This requires that the corrector be iterated on or that the error be monitored at every step.

(3) By iterating on the corrector, instability may result.

The Hamming predictor-corrector has advantages as follows:

(1) Error estimate is available at every step.

(2) The method is not implicit and, thus, requires no iterations.

The disadvantages are:

(1) The method, like Adams-Moulton, is not self-starting.

(2) Four calculations, two more than Adams-Moulton, are required per step.

5.3 Recommendations for Further Study

By expanding on the work done in this thesis, many areas of further research could be explored. It would be beneficial to extend the work done here to larger systems. While it may be safe to extrapolate the conclusions of this work to larger systems, these conclusions should be confirmed.

An important area for further study is the effect of higher order models, for each generator, on the results. The inclusion of governor, turbine, and excitation controls will produce a model of order greater than two. The higher order system thus produces more differential equations for each machine studied. Since the model will be of order greater than two, it is probable that a closed form solution for state transition cannot be obtained. If this is the case, it would be necessary to calculate the $\underline{\phi}$ and $\underline{\theta}$ matrices using a power series expansion. The use of the power series would cause a loss in speed of solution time but would probably not result in too great a loss of accuracy. It would also be interesting to note the effects of a higher order system on the other four algorithms.

From the results obtained, it appears that the trapezoidal rule has potential. Work could be done in the area of simultaneous solution of the algebraic and differential equations using the trapezoidal rule [6]. It may also prove useful to modify the existing program so that, as the solution of $\underline{x}_{n+1}$ is iterated on, the value of the accelerating power is calculated every second or third iteration instead of every iteration as it was for this thesis. Since, on the average, five or six iterations were required at every step, this should result in a significant time savings without a loss of accuracy. Newton Raphson iterative techniques should also be explored.

Another intersting area of study would be to employ some combination of state transition and the trapezoidal rule. The trapezoidal rule could be used to solve the forced part of the response and state transition to solve the unforced response. By using the trapezoidal rule, the clamping

approximation used in state transition would become a linear approximation.

Studies in the area of the predictor-corrector methods could include the effects of using state transition to provide the starting values for the predictor-corrector. The high accuracy provided by state transition may improve the accuracy of the predictor-corrector.

In a recent thesis by Gracia [20], dynamic load modeling was implemented in the stability problem. A combination of dynamic load modeling and the work done in this thesis might produce some interesting results. Therefore, such a study warrants careful consideration.

REFERENCES

[1] S. D. Conte and C. DeBoor, Elementary Numerical Analysis, 2nd Ed., McGraw-Hill, New York, N.Y., 1972.

[2] O. I. Elgerd, Electric Energy Systems Theory: An Introduction, McGraw-Hill, New York, N.Y., 1971.

[3] J. A. Jacquez, A First Course in Computing and Numerical Methods, Addison-Wesley, Reading, Mass., 1970.

[4] W. D. Humpage and B. Stott, "Predictor-Corrector Methods of Numerical Integration in Digital-Computer Analyses of Power-System Transient Stability", Proc. IEE, Vol. 112, pp. 1557-1565, August 1965.

[5] M. M. Adibi, P. M. Hirsch and J. A. Jordan, Jr., "Solution Methods for Transient and Dynamic Stability", Proc. IEEE, Vol. 62, pp. 951-958, July 1974.

[6] H. W. Dommel, N. Sato, "Fast Transient Stability Solutions", IEEE Trans. on P.A.S., pp. 1643-1650, July/August, 1972.

[7] H. L. Fuller, P. M. Hirsch and M. B. Lambie, "Variable Integration Step Transient Analysis", 1973 PICA Conference Proc., pp. 277-284, 1973.

[8] P. M. Anderson and A. A. Fouad, Power System Control and Stability, The Iowa State University Press, Ames, Iowa, 1977.

[9] G. W. Stagg and A. H. El-Abiad, Computer Methods in Power System Analysis, McGraw-Hill, New York, 1968.

[10] G. Gross and A. R. Bergen, "A Class of New Multistep Integration Algorithms for the Computation of Power System Dynamical Response", IEEE Trans. on P.A.S., Vol. PAS-96, pp. 293-300, Jan/Feb. 1977.

[11] F. Plitman Z. and M. Iza L., "Transient Stability Problem Solution Using the Hamming Predictor-Corrector Method", IEEE Trans., Vol. PAS-91, pp. 1371-1378, July/August 1972.

[12] K. N. Stanton and S. N. Talukdar, "New Integration Algorithms for Transient Stability Studies", IEEE Trans. on P.A.S., Vol. PAS-89, pp. 985-991, May/June 1970.

[13] S. N. Talukdar, "Iterative Multistep Method for Transient Stability Studies", Trans. on P.A.S., Vol. PAS-90, pp. 96-102, Jan/Feb. 1971.

[14] L. L. Grigsby, "A Transient Stability Algorithm", Unpublished Lecture Notes, Virginia Polytechnic Institute and State University, 1976.

[15] G. B. Thomas, Jr., Calculus and Analytic Geometry, Alternate Edition, Addison-Wesley, Reading, Mass., 1972.

[16] North American Rockwell, "On-Line Stability Study", Edison Electric Institute Report, RP 90-1, 1970.

[17] M. Walker, "Power Systems Analysis on Programmable Calculators", Master's Thesis, Virginia Polytechnic Institute and State University, 1974.

[18] "AEP Standard Test Systems", American Electric Power Serivce Corporation, New York, N.Y., 1961.

[19] P. M. DeRusso, R. J. Roy and C. M. Close, State Variables for Engineers, John Wiley and Sons, New York, N.Y. 1965.

[20] J. R. Gracia, "Dynamic Load Modeling in Power System Analysis", Master's Thesis, Virginia Polytechnic Institute and State University, 1977.

APPENDIX A

L U Decomposition

L U decomposition is a solution technique used to solve

$$\underline{A}x = \underline{b}. \tag{A.1}$$

The direct solution of (A.1) is obtained by converting $\underline{A}$ into the product of $\underline{L}$, a lower triangular matrix, and $\underline{U}$, an upper triangular matrix.

Assume $\underline{A}$ is of the general form

$$\underline{A} = \begin{bmatrix} a_{11} & a_{12} & \cdots & a_{1n} \\ a_{21} & a_{22} & \cdots & a_{2n} \\ \vdots & \vdots & & \vdots \\ a_{n1} & a_{n2} & \cdots & a_{nn} \end{bmatrix}. \tag{A.2}$$

(Note: We will assume diagonal entries of $\underline{A}$ to be nonzero.)

The elements of $\underline{U}$ are obtained by performing Gauss elimination on $\underline{A}$ and the elements of $\underline{L}$ are the multiples used to obtain $\underline{U}$. To perform Gauss elimination, we must convert the subdiagonal entries of $\underline{A}$ to zero as follows:

(1) For $a_{21}^{(1)} = 0$ (the superscript 1 indicates operations performed on column 1),

(a) calculate multiplier $m_{21} = \dfrac{a_{21}}{a_{11}}$;

(b) multiply row 1 by m_{21} and subtract from row 2.

(2) For $a_{n1}^{(1)} = 0$,

(a) calculate multiplier $m_{n1} = \dfrac{a_{n1}}{a_{11}}$;

(b) multiply row 1 by m_{n1} and subtract from row n.

After performing operations on column one, we obtain the following modified version of $\underline{A}$

$$\underline{A}^{(1)} = \begin{bmatrix} a_{11} & a_{12} & \cdots & a_{1n} \\ 0 & a_{22}^{(1)} & \cdots & a_{2n}^{(1)} \\ \vdots & \vdots & & \vdots \\ 0 & a_{n2}^{(1)} & \cdots & a_{nn}^{(1)} \end{bmatrix}. \qquad (A.3)$$

Repeat similar operations on the subdiagonal elements of columns 2 through n. The Gauss eliminated $\underline{A}$ matrix will be of the form

$$\underline{A}' = \begin{bmatrix} a'_{11} & a'_{12} & \cdots & a'_{1n} \\ & a'_{22} & \cdots & a'_{2n} \\ & & \ddots & \vdots \\ & \underline{0} & & a'_{nn} \end{bmatrix}. \qquad (A.4)$$

The $\underline{U}$ matrix is equal to $\underline{A}'$ and the $\underline{L}$ matrix is

$$\underline{L} = \begin{bmatrix} 1 & & & \\ m_{21} & 1 & & \underline{0} \\ m_{31} & m_{32} & 1 & \\ \vdots & \vdots & & \ddots \\ m_{n1} & m_{n2} & \cdots & 1 \end{bmatrix} \qquad (A.5)$$

where the m_{ij}'s are the multipliers.

We now have the following form of (A.1)

$$\underline{L}\,\underline{U}\,\underline{x} = \underline{A}\,\underline{x} = \underline{b} \qquad (A.6)$$

To solve (A.6) we must solve the following auxiliary equations:

$$\underline{L}\,\underline{y} = \underline{b} \tag{A.7a}$$

$$\underline{U}\,\underline{x} = \underline{y} \tag{A.7b}$$

We can solve (A.7a) for $\underline{y}$ using forward elimination. Using this solution, $\underline{y}$, we solve (A.7b) for $\underline{x}$ using back substitution.

The desirability of $\underline{L}\,\underline{U}$ decomposition is that once $\underline{L}$ and $\underline{U}$ have been found, $\underline{x}$ can be solved for using any $\underline{b}$ vector. Since the $\underline{b}$ vector was not operated on, we can solve for the new $\underline{x}$ directly. (Note: If any diagonal element of $\underline{A}^{(k)}$ is zero, we must permute the rows of $\underline{A}^{(k)}$ and, thus, the rows of $\underline{b}$.) The $\underline{L}$ and $\underline{U}$ matrices can also be stored in a single matrix, thus reducing the storage requirements, as

$$\underline{L}\,\underline{U} = \begin{bmatrix} a'_{11} & a'_{12} & \cdots & a'_{1n} \\ m_{21} & a'_{22} & \cdots & a'_{2n} \\ \vdots & \vdots & & \vdots \\ m_{n1} & m_{n2} & \cdots & a'_{nn} \end{bmatrix}. \tag{A.8}$$

Recall that the diagonal elements of $\underline{L}$ are one (1).

VITA

Edward Carter Gibson was born in Suffolk, Virginia, on August 12, 1954, the son of Mr. and Mrs. George T. Gibson. He graduated from Loudoun County High School in June 1972, and entered Virginia Polytechnic Institute and State University, Blacksburg, Virginia, that fall. He received his Bachelor of Science in Electrical Engineering in June 1976.

He then entered graduate school at VPI & SU to work toward a Master of Science in Electrical Engineering. During his graduate studies, he worked as a research assistant for the Energy Research Group under Dr. L. L. Grigsby. He received his M.S. in December 1977.

In August 1976, he married Rhonda King of Monterey, Virginia.

E. Carter Gibson

Edward Carter Gibson

A COMPARISON OF NUMERICAL ALGORITHMS FOR SOLUTION OF THE TRANSIENT STABILITY PROBLEM

by

E. Carter Gibson

(ABSTRACT)

A comparison is presented of five different numerical algorithms for the solution of the differential equations contained in the transient stability problem. A classical transient stability model is used, including the swing equation to characterize the machine's dynamic behavior. The five algorithms studied are: fourth-order Runge-Kutta; state transition; the trapezoidal rule; Adams-Moulton predictor-corrector; and Hamming predictor-corrector.

The five algorithms, using various step sizes, are applied to three test systems, including the IEEE 14-bus system, using a commom main program to call each algorithm as an independent subroutine. The results obtained are compared with regard to accuracy, solution time, and ease of programming. The comparison of fourth-order Runge-Kutta to the other methods is given special emphasis.